AMERICAN SOCIETY FOR MICROBIOLOGY | Journal of Virology®

PATHOGENESIS AND IMMUNITY

# A Dual Motif in the Hemagglutinin of H5N1 Goose/Guangdong-Like Highly Pathogenic Avian Influenza Virus Strains Is Conserved from Their Early Evolution and Increases both Membrane Fusion pH and Virulence

**Ute Wessels,[a] Elsayed M. Abdelwhab,[a] Jutta Veits,[a] Donata Hoffmann,[b] Svenja Mamerow,[a] Olga Stech,[a] Jan Hellert,[c] Martin Beer,[b] Thomas C. Mettenleiter,[a] Jürgen Stech[a]**

[a]Institute of Molecular Virology and Cell Biology, Friedrich Loeffler Institut, Federal Research Institute for Animal Health, Greifswald-Insel Riems, Germany

[b]Institute of Diagnostic Virology, Friedrich Loeffler Institut, Federal Research Institute for Animal Health, Greifswald-Insel Riems, Germany

[c]Institut Pasteur, Département de Virologie, Unité de Virologie Structurale, Paris, France

**ABSTRACT** Zoonotic highly pathogenic avian influenza viruses (HPAIV) have raised serious public health concerns of a novel pandemic. These strains emerge from low-pathogenic precursors by the acquisition of a polybasic hemagglutinin (HA) cleavage site, the prime virulence determinant. However, required coadaptations of the HA early in HPAIV evolution remained uncertain. To address this question, we generated several HA1/HA2 chimeras and point mutants of an H5N1 clade 2.2.2 HPAIV and an H5N1 low-pathogenic strain. Initial surveys of 3,385 HPAIV H5 HA sequences revealed frequencies of 0.5% for the single amino acids 123R and 124I but a frequency of 97.5% for the dual combination. This highly conserved dual motif is still retained in contemporary H5 HPAIV, including the novel H5NX reassortants carrying neuraminidases of different subtypes, like the H5N8 and the zoonotic H5N6 strains. Remarkably, the earliest Asian H5N1 HPAIV, the Goose/Guangdong strains from 1996/1997, carried 123R only, whereas 124I appeared later in 1997. Experimental reversion in the HPAIV HA to the two residues 123S and124T, characteristic of low-pathogenic strains, prevented virus rescue, while the single substitutions attenuated the virus in both chicken and mice considerably, accompanied by a decreased HA fusion pH. This increased pH sensitivity of H5 HPAIV enables HA-mediated membrane fusion at a higher endosomal pH. Therefore, this HA adaptation may permit infection of cells with less-acidic endosomes, e.g., within the respiratory tract, resulting in an extended organ tropism. Taken together, HA coadaptation to increased acid sensitivity promoted the early evolution of H5 Goose/Guangdong-like HPAIV strains and is still required for their zoonotic potential.

**IMPORTANCE** Zoonotic highly pathogenic avian influenza viruses (HPAIV) have raised serious public health concerns of a novel pandemic. Their prime virulence determinant is the polybasic hemagglutinin (HA) cleavage site. However, required coadaptations in the HA (and other genes) remained uncertain. Here, we identified the dual motif 123R/124I in the HA head that increases the activation pH of HA-mediated membrane fusion, essential for virus genome release into the cytoplasm. This motif is extremely predominant in H5 HPAIV and emerged already in the earliest 1997 H5N1 HPAIV. Reversion to 123S or 124T, characteristic of low-pathogenic strains, attenuated the virus in chicken and mice, accompanied by a decreased HA activation pH. This increased pH sensitivity of H5 HPAIV extends the viral tropism to cells with less-acidic endosomes, e.g., within the respiratory tract. Therefore, early HA

**Received** 8 May 2018 **Accepted** 2 June 2018

**Accepted manuscript posted online** 13 June 2018

**Citation** Wessels U, Abdelwhab EM, Veits J, Hoffmann D, Mamerow S, Stech O, Hellert J, Beer M, Mettenleiter TC, Stech J. 2018. A dual motif in the hemagglutinin of H5N1 Goose/Guangdong-like highly pathogenic avian influenza virus strains is conserved from their early evolution and increases both membrane fusion pH and virulence. J Virol 92:e00778-18. https://doi.org/10.1128/JVI.00778-18.

**Editor** Stacey Schultz-Cherry, St. Jude Children's Research Hospital



Address correspondence to Jürgen Stech, juergen.stech@fli.de.

adaptation to increased acid sensitivity promoted the emergence of H5 Goose/Guangdong-like HPAIV strains and is required for their zoonotic potential.

**KEYWORDS** influenza virus, H5N1, virus evolution, HPAIV, hemagglutinin, HA

Highly pathogenic avian influenza viruses (HPAIV) cause enormous losses in poultry worldwide and have raised concerns about a novel pandemic due to repeated zoonotic transmissions to humans (1). HPAIV emerge from low-pathogenic precursors after circulation in poultry (2–5) by an extension of the common monobasic hemagglutinin (HA) cleavage site (HACS) to a polybasic motif (6–8). To mediate membrane fusion between the virion and endosome, the HA has to be activated by proteolytic cleavage (9–11). The precursor protein HA0 is cleaved into the HA1 (head) and HA2 (stem) fragments by several host proteases whose recruitment depends on the HACS motif. Whereas the monobasic HACS prevalent in low-pathogenic avian influenza viruses (LPAIV) and seasonal human strains is susceptible to proteases like TMPRSS2 and HAT (12), HPAIV carry a polybasic HACS that is susceptible to ubiquitous furin (13), permitting systemic viral spread. Except for one H4 LPAIV (14), so far, polybasic HACS are naturally confined to HA subtype H5 or H7. Because experimental reversion to a monobasic motif abolishes virulence (15, 16), the polybasic HACS is considered the prime virulence determinant in HPAIV (6, 8, 16, 17). In contrast, conversion of the monobasic HACS of an LPAIV to a polybasic motif does not result in a highly pathogenic phenotype in most cases (15, 18–21). Those two findings reveal the existence of additional virulence determinants (15, 18, 20). An increase in virulence was already attributed to the PB2, PB1, NP, neuraminidase (NA) (in particular the stalk deletion), M, and NS genes (22–28). In this study, we focused on novel virulence determinants within the HA. Following receptor binding, depending on the cellular receptor specificity (29–32), HA mediates the fusion of the virion envelope with the endosomal membrane (9, 33, 34). The activation of fusion competence requires a conformational change of HA that is triggered at a particular pH (35). Remarkably, the pH values required for this essential HA rearrangement differ considerably among different influenza virus strains. In human strains, the HA-activating pH values appear to decrease with adaptation to the human host (36). In contrast, among avian strains, LPAIV generally display a lower activating pH, whereas contemporary H5 HPAIV exhibit a higher pH (37). These different activating pH are likely involved in virulence and host adaptation.

## RESULTS

**The dual motif 123R/124I is predominant in hemagglutinins of H5 HPAIV.** To reveal differences in the HA proteins of H5 LPAIV and HPAIV, we surveyed the fluDB (38) and GISAID (https://www.gisaid.org/) public databases. For analysis, we included 4,188 aligned sequences to generate the consensus HA sequences from LPAIV (803 entries) and HPAIV (3,385 entries). They differ by 35 amino acid exchanges in HA1 and by 8 exchanges in HA2 (Fig. 1). As parental viruses for the generation of HA mutants by reverse genetics (39), we used the recombinant H5N1 HPAIV A/Swan/Germany/R65/06 (R65) (17) and the polybasic HA cleavage site mutant (TG05-$HA_{poly}$) of H5N1 LPAIV A/Teal/Germany/Wv632/2005 (TG05) (18). Their HA sequences and the consensus sequences from LPAIV and HPAIV share 22 amino acid exchanges in HA1 and 5 exchanges in HA2 (Fig. 1), narrowing the range of relevant mutations in the HA.

The substitution T124I reduces acid stability accompanied by differentially increased virulence in chicken (37) (corresponding to position 108 in that study). Strikingly, within the HPAIV HA consensus sequence, including the R65 HA (Fig. 1), the preceding amino acid residue S123 was altered to R. In contrast to LPAIV, in which positions 123 and 124 contain S and T in 93.8% of sequences, in HPAIV, both residues are replaced by R and I in 97.5% of sequences (Fig. 2A). Furthermore, R65 carries an incomplete potential N-glycosylation motif (40) due to R at position 156 (Fig. 1). In most H5 HPAIV (80.4%) (38) (https://www.gisaid.org/), this motif is incomplete (Fig. 2B). Whereas its absence is crucial for high virulence

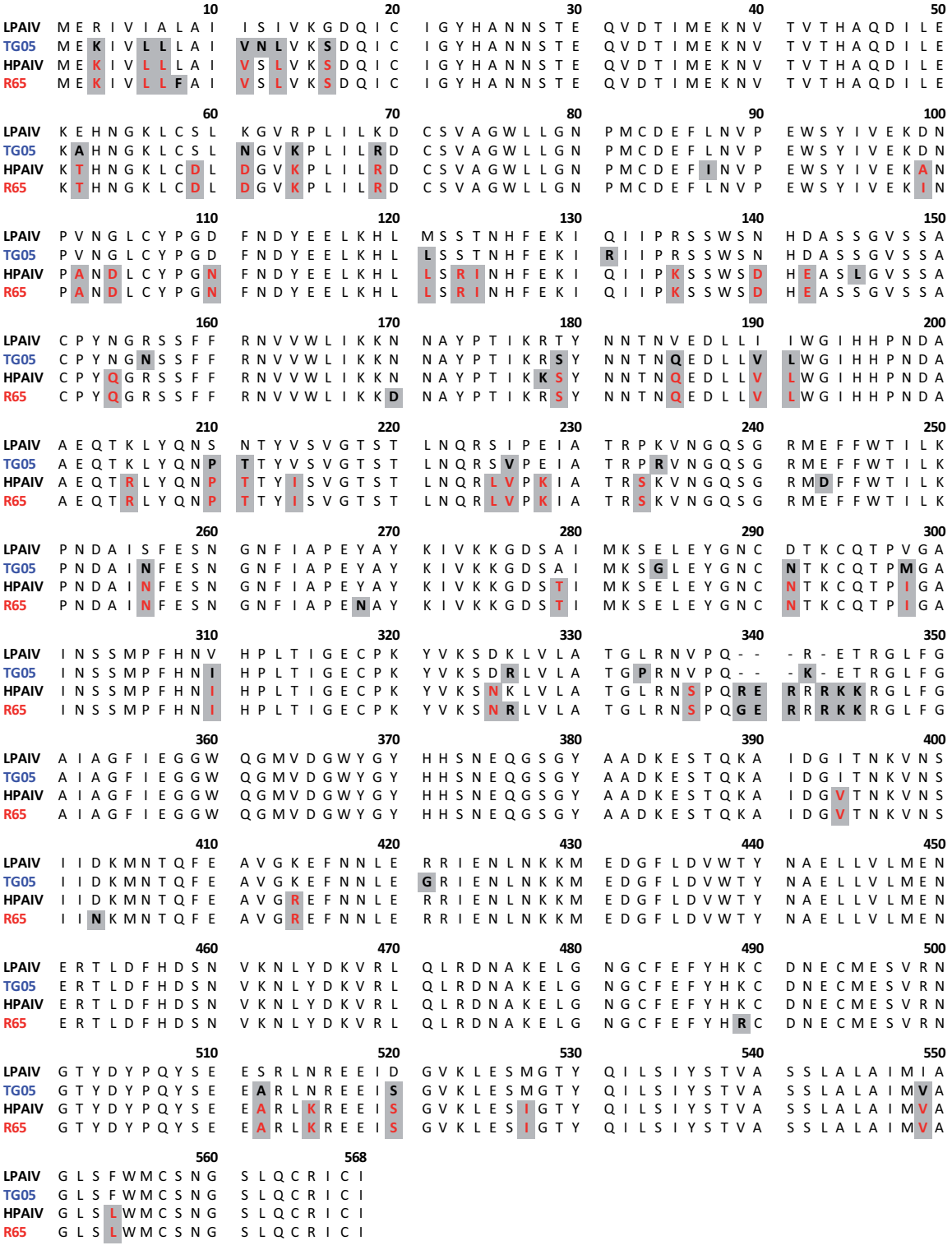


**FIG 1** Alignment of consensus sequences of the HA proteins from LPAIV, TG05, HPAIV, and R65. For analysis, we surveyed the fluDB (38) and GISAID (https://www.gisaid.org/) public databases and included 4,188 full-length aligned sequences to generate the consensus HA sequences from LPAIV (803 entries) and HPAIV (3,385 entries).

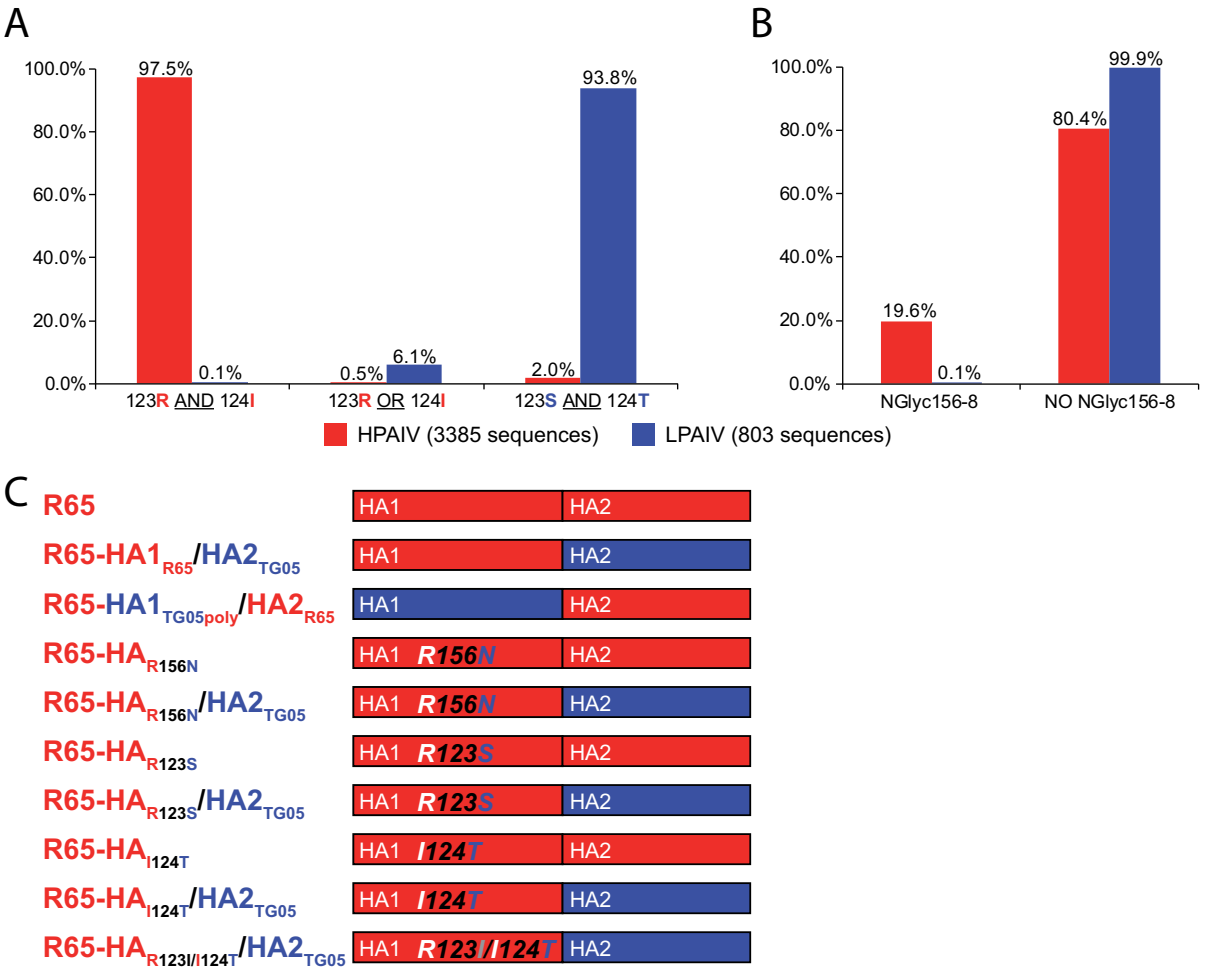


**FIG 2** Frequencies of the dual motif 123R/124I (A) and the N-glycosylation motif spanning residues 156 to 158 (B) in H5 HPAIV and generated recombinant viruses (C). Shown are frequencies of amino acids at positions 123 and 124 (A) or an N-glycosylation motif at positions 156 to 158 (B) within H5 HA of HPAIV and LPAIV among 4,188 protein sequences downloaded from the fluDB (38) and GISAID (https://www.gisaid.org/) public databases on 24 July 2017. Positions refer to the R65 HA, including the signal peptide.

and contact transmission in mammalian models (40, 41), its phenotype in chicken is unknown.

Taken together, the sequence survey indicates that position 156 and in particular the dual motif at positions 123 and 124 are candidate virulence determinants in H5 HPAIV.

**HA 123R and 124I form a coupled motif crucial for fitness of R65.** To investigate the impact of all amino acid exchanges in the entire HA1 and HA2 regions beside the dual motif 123R/124I, we first constructed HA chimeric viruses by replacing the HA1 or HA2 part in R65 with that of TG05-$HA_{poly}$, resulting in the HA chimeras R65-$HA1_{TG05poly}$/$HA2_{R65}$ and R65-$HA1_{R65}$/$HA2_{TG05}$, respectively (Fig. 2C).

According to our surveys using sequence databases, we introduced three TG05 amino acid residues into R65 HA1, resulting in the mutants R65-$HA_{R156N}$, R65-$HA_{R123S}$, and R65-$HA_{I124T}$ (Fig. 2C). Remarkably, we could not rescue a double-virus mutant carrying both R123S and I124T in the authentic R65 HA. We speculate that this result is due to severely impaired fitness.

We also introduced the same HA1 point mutations into the HA2 chimera R65-$HA1_{R65}$/$HA2_{TG05}$, resulting in R65-$HA_{R156N}HA2_{TG05}$, R65-$HA_{R123S}HA2_{TG05}$, R65-$HA_{I124T}HA2_{TG05}$, and R65-$HA_{R123S+I124T}$/$HA2_{TG05}$ (Fig. 2C).

After a first passage of the rescued viruses on MDCK cells, we also found the acquired HA mutations M405I in R65-$HA1_{TG05poly}$/$HA2_{R65}$, G217W in R65-$HA_{R123S}$,

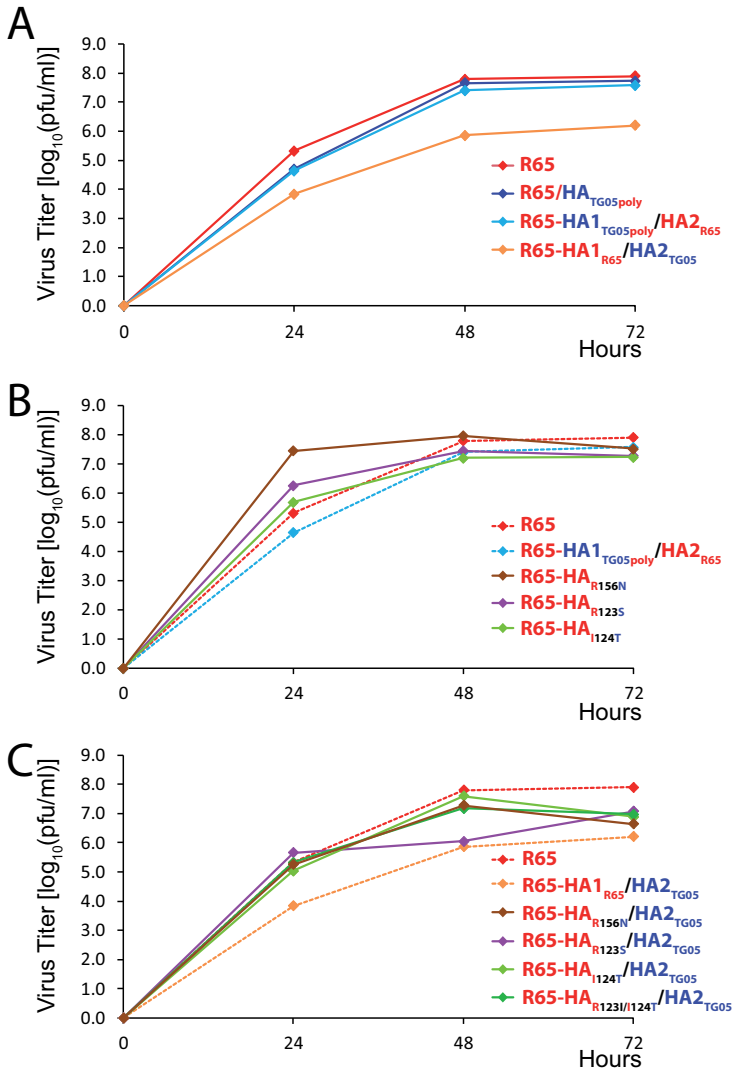


**FIG 3** Growth curves. We inoculated DF1 cells with virus at a multiplicity of infection of $10^{-3}$ in duplicate and determined the average titers at the respective time points by plaque assays. In panels B and C, the growth curves for R65, R65-HA1$_{TG05poly}$/HA2$_{R65}$, and R65-HA1$_{R65}$/HA2$_{TG05}$ are identical to those from panel A and are included for comparison (dotted lines).

and S123I in R65-HA$_{R123S+I124T}$HA2$_{TG05}$, which we therefore renamed R65-HA$_{R123I+I124T}$HA2$_{TG05}$. This finding of a pseudoreversion in the latter HA chimera corresponds to our failure to rescue the R65 nonchimeric position 123/124 double mutant. Taken together, these results indicate that the two amino acid residues R123 and I124 within HA1 form a coupled motif, which is crucial for the fitness of an H5N1 HPAIV like R65.

**No impaired replication efficiency of the R65 mutants *in vitro*.** To study the impact of the HA mutations on replication efficiency, we determined growth curves on DF1 cells. The HA2$_{TG05}$ chimera R65-HA1$_{R65}$/HA2$_{TG05}$ exhibited a replication kinetic that was decreased by 2 orders of magnitude compared to the parental R65, the TG05 HA reassortant R65-HA$_{TG05poly}$, and the HA1$_{TG05}$ chimera R65-HA1$_{TG05poly}$/HA2$_{R65}$ (Fig. 3A). All viruses with the HA1 region modified, such as R65-HA1$_{TG05poly}$/HA2$_{R65}$ or the single point mutant R65-HA$_{R156N}$, R65-HA$_{R123S}$, or R65-HA$_{I124T}$, and wild-type R65 displayed titers within 1 order of magnitude at 48 h postinfection (p.i.). However, R65-HA$_{R156N}$ came close to its maximum already at 24 h p.i. (Fig. 3B). In contrast to R65-HA1$_{R65}$/HA2$_{TG05}$, which replicated approximately 100-fold less than R65, all the other HA2$_{TG05}$

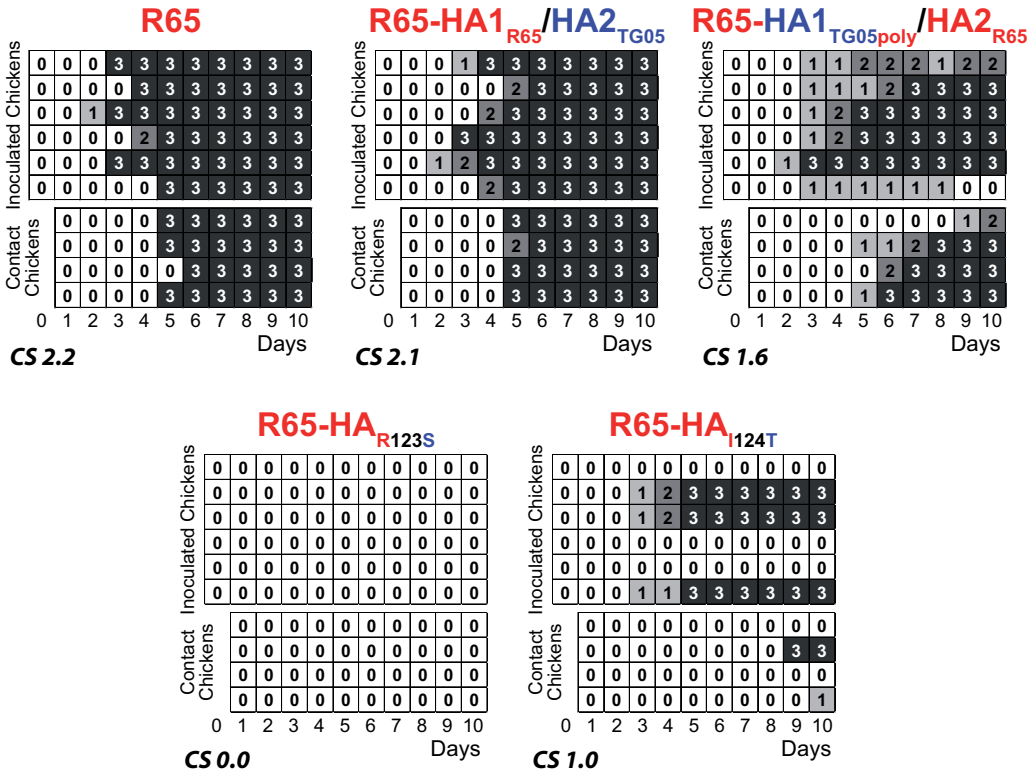


**FIG 4** HA1 R123S and I124T exchanges abolish or reduce virulence in chicken. We infected the birds oculonasally with $10^5$ PFU virus and added contact animals on day 1 p.i. Daily individual clinical scores were 0 for healthy, 1 for ill, 2 for severely ill, and 3 for dead. CS, total clinical score for the whole group of the primarily infected (inoculated) chickens.

chimeras carrying an additional TG05 point mutation within HA1 displayed a replication efficiency similar to that of R65: R65-$HA_{R156N}$/$HA2_{TG05}$, R65-$HA_{R123S}$/$HA2_{TG05}$, R65-$HA_{I124T}$/$HA2_{TG05}$, or R65-$HA_{R123I+I124T}HA2_{TG05}$ (Fig. 3C). Taken together, HA2 replacement, as with R65-$HA1_{R65}$/$HA2_{TG05}$, led to a titer reduction, which, however, is offset by any of the HA1 point mutations from TG05. Furthermore, we observed no apparent growth disadvantage of the R65 mutants in DF1 cells in the case of HA1 replacement or one of the R123S and I124T substitutions.

**The HA R123S and I124T mutations strongly attenuate HPAIV R65 in chicken.** To investigate the virulence and transmission of R65, R65-$HA1_{R65}$/$HA2_{TG05}$, R65-$HA1_{TG05poly}$/$HA2_{R65}$, R65-$HA_{R123S}$, and R65-$HA_{I124T}$ in chicken, we infected six birds per group oculonasally with $10^5$ PFU and added four contact chickens at day 1 p.i. All birds infected with R65 or R65-$HA1_{R65}$/$HA2_{TG05}$, including the contact animals, succumbed to death, whereas among the R65-$HA1_{TG05poly}$/$HA2_{R65}$-infected chickens, two primarily infected birds and one contact bird survived (Fig. 4). Those two primarily infected birds displayed clinical symptoms from day 3 p.i., one recovered until day 9 p.i., and both animals seroconverted (data not shown). The surviving contact animal developed mild symptoms on day 9 p.i. and was still seronegative on day 10 p.i. In contrast, virulence and transmissibility were reduced drastically for R65-$HA_{R123S}$ and R65-$HA_{I124T}$; all animals remained seronegative. Infection with the latter resulted in death of three primarily infected animals and one contact bird. Another contact bird developed mild symptoms on day 10 p.i. and was seronegative at that time. R65-$HA_{R123S}$ did not cause any clinical symptoms or seroconversion in primarily infected or contact animals (Fig. 4).

For investigation of the point mutants and HA2 chimeras R65-$HA_{R156N}$, R65-$HA_{R156N}$/$HA2_{TG05}$, R65-$HA_{R123S}$/$HA2_{TG05}$, R65-$HA_{I124T}$/$HA2_{TG05}$, and R65-$HA_{R123I+I124T}$/$HA2_{TG05}$, we infected three chickens per group oculonasally. All animals died, with total clinical scores ranging from 2.0 to 2.2, close to that of R65, with a score of 2.2. Only R65-$HA_{R156N}$ displayed a slightly increased value of 2.6 (Fig. 4 and Table 1). Therefore, the replace-

**TABLE 1** Virulence of HA point mutants and chimeras in chickens[a]

| Virus | No. of dead chickens/total no. of chickens | Clinical score |
|---|---|---|
| R65-HA$_{R156N}$ | 3/3 | 2.6 |
| R65-HA$_{R156N}$HA2$_{TG05}$ | 3/3 | 2.0 |
| R65-HA$_{R123S}$HA2$_{TG05}$ | 3/3 | 2.1 |
| R65-HA$_{I124T}$HA2$_{TG05}$ | 3/3 | 2.1 |
| R65-HA$_{R123I+I124T}$HA2$_{TG05}$ | 3/3 | 2.2 |

[a]Mortality rates and clinical scores were determined after oculonasal infection with $10^5$ PFU of the inoculum virus. Clinical scores were 0 for healthy, 1 for ill, 2 for severely ill, and 3 for dead.

ment of R65 HA2 by that of TG05 can restore the virulent phenotype even in the presence of the point mutations R123S and I124T. Overall, the strong attenuation of R65 in the presence of the two HA mutations R123S and I124T in chicken demonstrates their crucial role in the virulence of HPAIV.

**HA R123S strongly attenuates R65 in mice.** To address the impact of the most attenuating mutation, HA R123S, in a mammalian model, we intranasally inoculated five mice per group with phosphate-buffered saline (PBS) or $10^4$ PFU of R65 or R65-HA$_{R123S}$. Whereas all R65-infected animals succumbed to death, the mock- and R65-HA$_{R123S}$-infected animals remained unaffected (Fig. 5A). To determine the viral titers in organs by a plaque assay, we infected mice and sacrificed them on day 3. In R65-infected mice ($n = 3$), we found high viral loads in lungs and hearts and a notable titer in the brain of one animal. However, in the R65-HA$_{R123S}$-infected mice ($n = 4$), we detected no lung titers in two animals or titers considerably reduced by 4 to 2 orders of magnitude in the

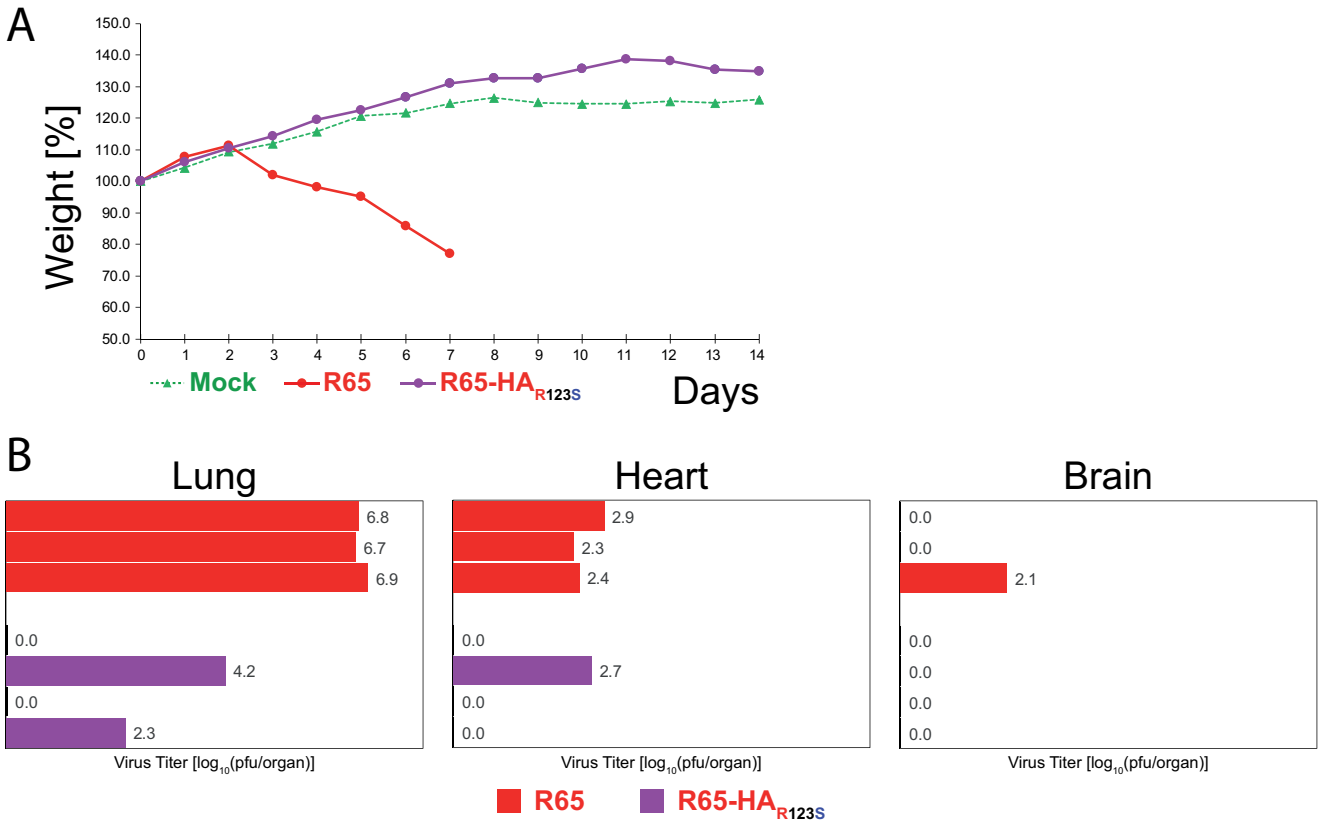


**FIG 5** HA1 exchange R123S abolishes virulence and reduces virus load in organs of mice. (A) Average body weights of 4-week-old female BALB/c mice inoculated intranasally with mock (PBS), R65, or R65-HA$_{R123S}$ ($n = 5$) at a dosage of $10^4$ PFU. Animals with weight losses of 25% or more were euthanized. All R65-infected mice died, whereas all R65-HA$_{R123S}$-infected animals remained unaffected throughout the experiment. (B) Organ titers, determined by plaque assays, from entire lungs, hearts, and brains taken on day 3 after intranasal inoculation with $10^4$ PFU of R65 or R65-HA$_{R123S}$. If necessary, titration began with undiluted homogenates.

**TABLE 2** Amino acid exchanges in HA and M2 proteins of virus in chicken and mouse[a]

| Virus | Total no. of animals | Animal | Day p.i. | Mutation | Description |
|---|---|---|---|---|---|
| Oral swabs from chickens | | | | | |
| R65-HA1$_{R65}$/HA2$_{TG05}$ | 10 | P-4 | 3 | HA I394G | V in R65 |
| | | C-1 | 3 | | |
| R65-HA$_{R156N}$/HA2$_{TG05}$ | 3 | P-3 | 6 | HA G421R | R in R65 |
| R65-HA$_{R123S}$/HA2$_{TG05}$ | 3 | P-3 | 6 | HA S123R | R in R65 |
| R65-HA$_{I124T}$/HA2$_{TG05}$ | 3 | P-2 | 3 | M2 R45L | —[b] |
| R65-HA$_{R123I+I124T}$/HA2$_{TG05}$ | 3 | P-1 | 3 | M2 D44N | —[b] |
| | | P-2 | 6 | M2 D44N | |
| | | P-3 | 3 | M2 R45L | —[b] |
| Reisolated virus from mouse heart homogenate | | | | | |
| R65-HA$_{R123S}$ | | Mouse | 3 | M2 R45H | —[b] |

[a]Primarily infected chickens are indicated with P, and contact birds are indicated with C. Positions of HA mutations refer to positions equivalent to those in R65.
[b]M2 amino acid residues D44 and R45 are highly conserved (21).

other two animals, a noticeable titer in the heart of one mouse, and no titers in the brains (Fig. 5B). Taken together, the HA R123S mutation in the clade 2.2.2 virus R65 (H5N1) abolishes virulence in both avian and mammalian hosts.

**HA R123S and I124T enforce compensatory HA and M2 mutations in chickens and mice.** Among positive PCR samples from oral swabs from infected chickens, we found the following HA changes. R65-HA1$_{R65}$/HA2$_{TG05}$ acquired the I394G exchange in the HA2 region; at this position, R65 carries V. Another HA2 mutation was found in shed R65-HA$_{R156N}$/HA2$_{TG05}$, G421R, being identical in HA2 of R65 (Table 2). Therefore, both chimeric viruses appear to adapt their heterologous HA2 part, originating from TG05, to R65 HA1. Moreover, R65-HA$_{R123S}$/HA2$_{TG05}$ reverted to S123R (Table 2). Furthermore, in R65-HA$_{I124T}$/HA2$_{TG05}$ and R65-HA$_{R123I+I124T}$/HA2$_{TG05}$, we found mutations in the exit region of the proton channel M2 (42–45), D44N and R45L (Table 2), indicating enforced coadaptation to the HA mutations at positions 123 and 124.

From the R65-HA$_{R123S}$-infected mouse displaying the highest virus titers (Fig. 5B), we reisolated virus from the heart and sequenced the HA and M genes. Whereas the introduced HA R123S exchange remained unaffected, M2 displayed the R45H exchange. Taken together, these observations support the notion that the HA1 R123S exchange plus the HA1 and HA2 parts from TG05 are incompatible with the R65 background and therefore entail compensatory mutations in HA or M2.

**Increased acid sensitivity of the R65 HA is paralleled by high virulence due to 123R/124I.** To determine the activation pH, enabling HA-mediated fusion, of each virus, we performed syncytium formation assays, whereas we assessed the acid stability in the environment by measurement of the virus inactivation pH (Fig. 6A). HPAIV R65 displays a high fusion activation pH of 5.9 and an inactivation pH of 5.7. However, TG05-HA$_{poly}$, which is an HACS mutant of LPAIV TG05 (18), has considerably lower pH values of 5.1 and 4.9, respectively. The introduction of the R65 HA into the TG05 background (TG05-HA$_{R65}$) resulted in increases of both pH values (5.8 and 5.4, respectively), but still below those of R65, suggesting the involvement of both HA and the other viral proteins. The reciprocal reassortant R65-HA$_{TG05poly}$ also displayed a lower fusion pH of 5.3 but an extremely low virus inactivation pH of 4.1. Furthermore, the replacement of the HA1 or HA2 regions decreased the pH values to different extents (R65-HA1$_{R65}$/HA2$_{TG05}$ and R65-HA1$_{TG05}$/HA2$_{R65}$). Restoration of the N-glycosylation site at positions 156 to 158 (R65-HA$_{R156N}$ and R65-HA$_{R156N}$/HA2$_{TG05}$) resulted in somewhat lower pH values, indicating enhanced stability. Remarkably, the HA R123S single mutation in R65 decreases the fusion activation pH from 5.9 to 4.9 and the virus inactivation pH from 5.7 to 4.4. Similarly, the I124T exchange leads to a decreased fusion activation pH of 5.6 and a virus inactivation pH of 4.7 (Fig. 6A). The introduction of TG05 HA2 changed the pH stability of all point mutants to various extents. Overall,

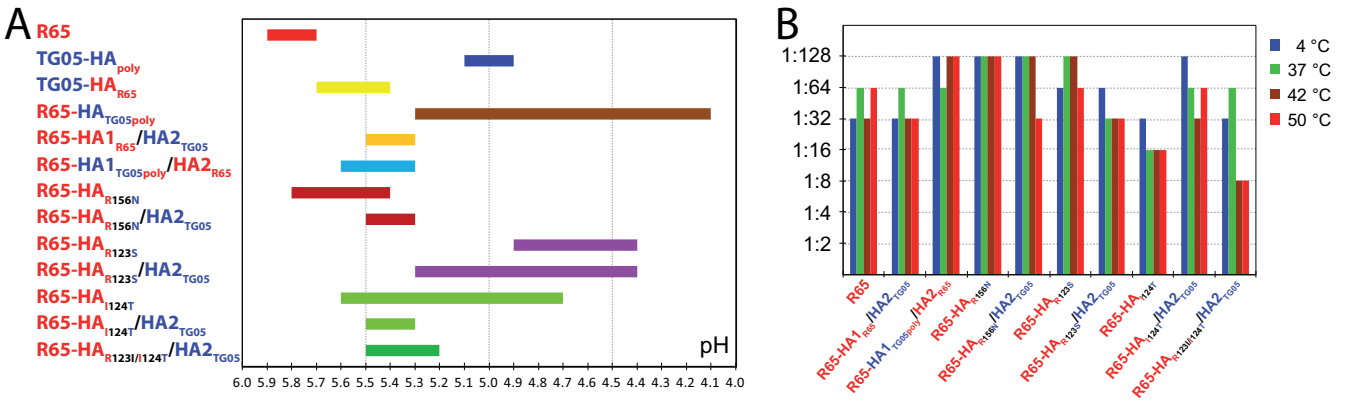


**FIG 6** Fusion activation pH and stability. (A) Decreased fusion activation pH and virus inactivation pH of HA chimeras and point mutants. For each virus, the left end of the bar indicates the fusion activation pH (the highest pH at which syncytia formed), whereas the right end represents the virus inactivation pH (the highest pH at which no cell infection was detectable). (B) Thermal stability of HA chimeras and point mutants. After incubation of the virus at the indicated temperatures for 30 min, we determined the HA titers at room temperature.

we found notable decreases of the fusion activation pH and virus inactivation pH in the presence of substitutions R123S and I124T.

Because an increased temperature may lead to fusion competence due to the spring-loaded metastable conformation of the HA (46), we investigated the influence of the HA mutations on thermal stability. To this end, we incubated R65 and all mutants at different temperatures for 30 min prior to an HA test. In contrast to all other viruses, R65-HA$_{R123I/I124T}$-HA2$_{TG05}$ displayed a reduced HA titer of 1:8 after incubation at 42°C, compared to an HA titer of 1:64 following incubation at 37°C (Fig. 6B). This result suggests that the TG05 HA2 part might destabilize the prefusion conformation of the HA from R65-HA$_{R123I/I124T}$-HA2$_{TG05}$ to some extent.

In general, for the virus variants studied, their virulence in chicken increased with their fusion activation pH (Fig. 7). In stark contrast to R65 and the N-glycosylation mutant R65-HA$_{R156N}$, displaying the highest clinical scores and pH values, the two single point mutants R65-HA$_{R123S}$ and R65-HA$_{I124T}$ have an avirulent or lower-pathogenicity phenotype accompanied by the lowest fusion activation pH. Therefore, an increased acid sensitivity of

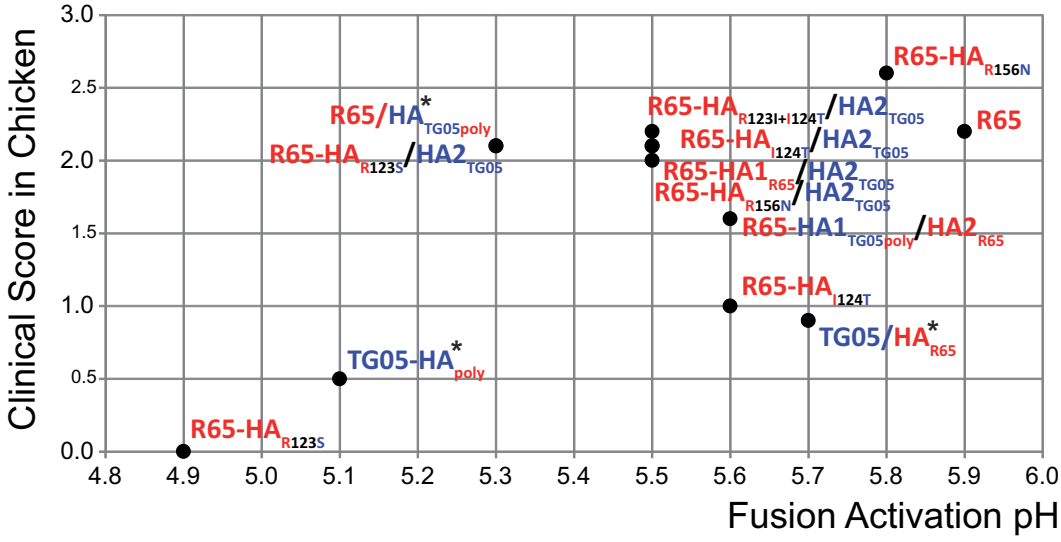


**FIG 7** Virulence in chickens increases with fusion activation pH. For each virus, the average clinical score in chickens is shown, along with the fusion activation pH determined by syncytium formation assays. Clinical scores are 0 for healthy, 1 for ill, 2 for severely ill, and 3 for dead. *, clinical scores of these viruses were determined previously (18).

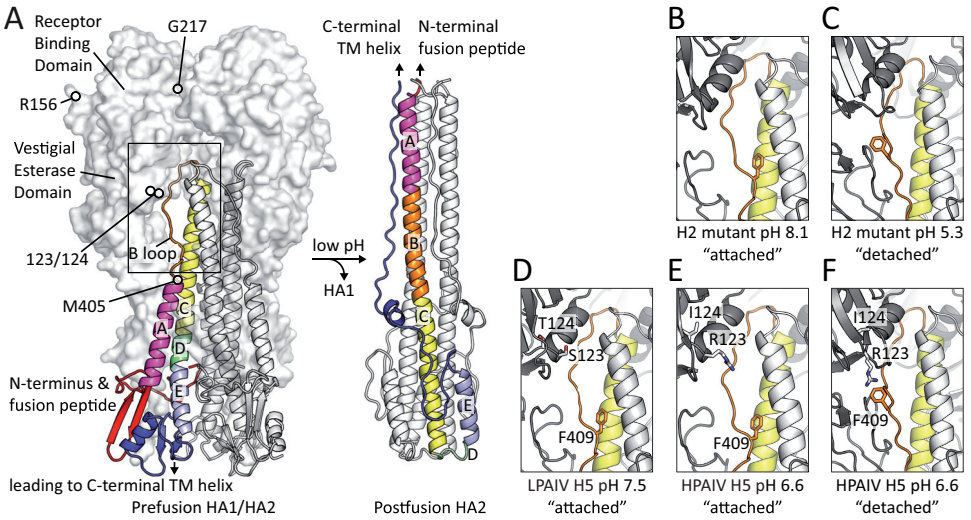


**FIG 8** Mechanistic implications for membrane fusion. (A) Prefusion conformation (PDB accession number 1JSM) (49) (left) and postfusion conformation (PDB accession number 4NKJ) (87) (right) of a hemagglutinin trimer. The HA1 subunit is shown in a transparent surface representation, and the HA2 subunit is shown in a cartoon representation. The different structural elements of a single HA2 protomer are highlighted in different colors. The rectangular outline indicates the region of close-ups in panels B to F. (B) The B loop conformation in a prefusion-stabilized mutant of A/Japan/305/1957 H2 at pH 8.1 (PDB accession number 3QQB) (47). (C) The same mutant at pH 5.3 (PDB accession number 3QQO) (47). (D) LPAIV A/duck/Singapore/3/1997 H5 at pH 7.5 (PDB accession number 1JSM) (49). (E) HPAIV A/Chicken/Hong Kong/YU562/01 H5 at pH 6.6 (PDB accession number 3S13) (37). (F) The same protein in another crystal form grown under identical conditions (PDB accession number 3S12) (37).

the HA is required for the high virulence of R65 mediated by the 123R/124I dual-amino-acid motif.

**Impact of 123R/124I on HA structure.** The fusion of virion and endosomal membranes results from the low-pH-triggered irreversible switch between the metastable "spring-loaded" prefusion conformation and the low-energy postfusion conformation of the HA. A key event during this process is the conversion of the B loop within the HA2 subunit into an $\alpha$ helix (Fig. 8A). Most available prefusion structures of H2, H5, and H6 hemagglutinins display similar conformations, in which the B loop is tightly attached to the central coiled coil of the HA2 stem (Fig. 8B). It has been suggested that early events in the conformational switch of these proteins involve a reversible detachment of the B loop from its prefusion position (47). The crystal structure of such an early fusion intermediate has been solved using a prefusion-stabilized mutant of the A/Japan/305/1957 H2 hemagglutinin at pH 5.3 (47) (Fig. 8C). Whereas the only three crystal structures of a canonical LPAIV H5 HA with the 123S/124T motif show the typical "attached" conformation of the B loop at pH 7.5 (48, 49) (Fig. 8D), some crystal structures of HPAIV H5 HA with the 123R/124I motif have the "detached" conformation of the B loop, even under neutral conditions, between pH 6.5 and pH 8.5 (37, 50–52). In contrast to A/Japan/305/1957 H2, where the initial detachment of the B loop appears to be low-pH dependent, the same process is therefore likely pH independent in HPAIV H5 hemagglutinins. For example, both conformations, the "attached" and the "detached" ones, were found in two different crystal forms of the same HPAIV H5 HA under identical crystallization conditions at pH 6.6 (37) (Fig. 8E and F). On the atomic level, the "detached" B loop within HA2 in the respective HPAIV H5 structures is held in suspension via multiple attractive interactions with the vestigial esterase domain of HA1. Of note, among the involved residues in the HA1 subunit is R123, which holds the benzene ring of F409 from the B loop via a cation-$\pi$ interaction (Fig. 8F). In light of these observations, we propose that R123 contributes to the destabilization of the HPAIV H5 prefusion conformation via pH-independent priming of the HA2 subunit for its conformational switch. Although the supporting role of I124 is less apparent from the

available structures, this residue likely affects the local structural dynamics of the vestigial esterase domain and thus influences the pH sensitivity of HPAIV H5 HA, as previously discussed (37).

## DISCUSSION

HPAIV arise from low-pathogenic precursor strains upon the acquisition of the polybasic HACS, the prime virulence factor (16). Its artificial introduction into the HA of low-pathogenic avian strains, however, does not necessarily lead to a highly pathogenic phenotype (15, 18–21), corresponding to the existence of further virulence determinants in other gene segments, such as in PB2, PB1, NP, M, or NA (22–28). Beyond that, the required coadaptation of the HA itself along with the acquisition of a polybasic HACS during early HPAIV evolution has remained uncertain. To this end, we generated a panel of HA mutants of clade 2.2.2 H5N1 HPAIV R65 (53) carrying HA1 or HA2 parts from H5N1 LPAIV TG05 (18) and/or several TG05 point mutations. We found that the R65 HA1 part and, in particular, the two HA amino acid residues 123R and 124I as a dual motif are required for extreme virulence in both chickens and mice.

After receptor-mediated endocytosis of the incoming virion along the endosomal pathway, the cleaved HA is subjected to a continuous pH decrease until an irreversible conformational change takes place that enables fusion of the membranes from the virion and endosome (9, 33, 34). A mild acidic fusion activation pH is common to HPAIV, in contrast to LPAIV (54), and regulates high virulence in chicken (37). In our study, we found that in R65, each of these two HA residues, 123R and 124I, is crucial for an elevated HA fusion activation pH.

After a first cell culture passage of our recombinant viruses, secondary HA mutations were acquired in R65-HA1$_{TG05poly}$/HA2$_{R65}$ (M405I), R65-HA$_{R123S}$ (G217W), and R65-HA$_{R123S+I124T}$/HA2$_{TG05}$ (S123I). The latter pseudoreversion of S123 to the larger side chain of an isoleucine clearly indicates the reduced fitness of the R123S/I124T double mutant on the R65 HA1 background. Moreover, the other two secondary mutations occurred at critical positions in the protein structure: M405 marks the N-terminal end of the B loop that connects it to $\alpha$ helix A (Fig. 8A). This region likely regulates the nucleation of $\alpha$ helix B during the conformational switch that triggers membrane fusion. G217, on the other hand, is located directly at the trimer interface in the receptor-binding domain of the HA1 subunit (Fig. 8A). Dissociation of HA1 is an essential step during the structural rearrangements promoting fusion. Both of these secondary mutations likely decrease the overall stability of the prefusion conformation and thus may partially compensate for the artificial introduction of our stabilizing mutations.

Furthermore, in viruses reisolated from chicken oral swabs and mouse heart homogenates, we found several mutations, such as the reversion HA S123R or HA2 mutations, in the TG05 HA2 chimeric viruses that were identical to or at the same positions as those in R65, indicating strong selection pressure. Moreover, we observed mutations in the M2 ion channel exit region (42, 44, 45, 55), D44N (43), R45L, and R45H, which were also selected in chickens infected with highly pathogenic reassortants carrying a non-H5/non-H7 HA (21). These mutations are prevalent in a few native HPAIV and LPAIV (21) and were demonstrated to compensate for the lower acid sensitivity of the HA (56).

The additional N-glycosylation motif formed by the R156N exchange in the HA of R65 resulted in somewhat increased growth properties, fusion activation pH, and virus inactivation pH and slightly increased virulence in chicken. Therefore, the very common loss of this N-glycosylation site in H5 HPAIV (Fig. 1 and 2B) is not detrimental in chickens. In contrast, its absence enhances virulence in mice, facilitates contact transmission in guinea pigs (40, 41), and is involved in airborne transmissibility in ferrets (57). Therefore, the absence of an N-glycosylation site at positions 156 to 158 might have supported the transit of the clade 2.2.2 viruses through some intermediate mammalian host(s) like, perhaps, pikas (58), as previously proposed for the mammalian marker mutation PB2 627K (59).

**TABLE 3** Chronological emergence of HA1 mutations[a]

| Virus Strains | Serotype | Accession | Year | 113 | 123 | 124 | 142 | 154 | 228 | 233 |
|---|---|---|---|---|---|---|---|---|---|---|
| H5 numbering without signal peptide* | | | | 97 | 107 | 108 | 126 | 138 | 212 | 217 |
| **Consensus H5 LPAIV** | | | | D | S | T | D | N | E | P |
| **Consensus H5 HPAIV** | | | | D | **R** | **I** | **E** | **Q** | **K** | **S** |
| A/Teal/Germany/WV632/2005 (TG05) | H5N1 | CY061885 | 2005 | D | S | T | D | N | E | P |
| A/Swan/Germany/R65/2006 (R65) | H5N1 | DQ464354 | 2006 | D | **R** | **I** | **E** | **Q** | **K** | **S** |
| A/Goose/Guangdong/1/1996 | H5N1 | AF144305 | 1996 | D | R | T | D | H | E | P |
| A/Goose/Guangdong/3/1997 | H5N1 | AF364334 | 1997 | D | R | T | D | H | E | P |
| A/Chicken/Hong Kong/220/1997 | H5N1 | AF046080 | 1997 | D | R | I | D | L | E | P |
| A/Hong Kong/156/1997 | H5N1 | AF046088 | 1997 | D | R | I | D | L | E | P |
| A/Hong Kong/483/1997 | H5N1 | AF046097 | 1997 | D | R | I | D | L | E | P |
| A/Chicken/Hong Kong/258/1997 | H5N1 | AF057291 | 1997 | D | R | I | D | L | E | P |
| A/Chicken/Hong Kong/728/1997 | H5N1 | AF046099 | 1997 | D | R | I | D | L | E | P |
| A/Chicken/Hong Kong/786/1997 | H5N1 | AF082035 | 1997 | D | R | I | D | L | E | P |
| A/Chicken/Hong Kong/Y385/1997 | H5N1 | AF098541 | 1997 | D | R | I | D | L | E | P |
| A/Chicken/Hubei/Wh/1997 | H5N1 | DQ997102 | 1997 | D | R | I | D | H | E | P |
| A/Chicken/Hubei/Wj/1997 | H5N1 | DQ997122 | 1997 | D | R | I | D | H | E | S |
| A/Chicken/Hubei/Wl/1997 | H5N1 | DQ997133 | 1997 | D | R | I | E | H | E | P |
| A/Duck/Hong Kong/P46/1997 | H5N1 | AF098543 | 1997 | D | R | I | D | L | E | P |
| A/Environment/Hong Kong/486/1997 | H5N1 | GU052035 | 1997 | D | R | I | D | L | E | P |
| A/Goose/Hong Kong/W355/1997 | H5N1 | AF098545 | 1997 | D | R | I | D | L | E | P |
| A/Hong Kong/482/1997 | H5N1 | AF046098 | 1997 | D | R | I | D | L | E | P |
| A/Hong Kong/485/1997 | H5N1 | GU052142 | 1997 | D | R | I | D | L | E | P |
| A/Silky Chicken/Hong Kong/P17/1997 | H5N1 | AF098546 | 1997 | D | R | I | D | L | E | P |
| A/Duck/Guangxi/07/1999 | H5N1 | AY585363 | 1999 | D | S | T | D | H | E | P |
| A/Environment/Hong Kong/43710/1999 | H5N1 | AF216737 | 1999 | N | R | T | D | H | E | P |
| A/Environment/Hong Kong/4374/1999 | H5N1 | AF216713 | 1999 | N | R | T | D | H | E | P |
| A/Environment/Hong Kong/4376/1999 | H5N1 | AF216721 | 1999 | N | R | T | D | H | E | P |
| A/Environment/Hong Kong/4378/1999 | H5N1 | AF216729 | 1999 | N | R | T | D | H | E | P |
| A/Goose/Hong Kong/4376/1999 | H5N1 | GU052019 | 1999 | N | R | T | D | H | E | P |
| A/Duck/Fujian/19/2000 | H5N1 | AY585359 | 2000 | D | R | I | D | H | E | P |
| A/Duck/Guangdong/07/2000 | H5N1 | AY585373 | 2000 | D | R | I | D | H | K | S |
| A/Duck/Guangdong/12/2000 | H5N1 | AY585361 | 2000 | D | R | I | D | H | E | P |
| A/Duck/Zhejiang/11/2000 | H5N1 | AY585371 | 2000 | D | R | I | D | H | E | P |
| A/Duck/Guangdong/40/2000 | H5N1 | AY585374 | 2000 | D | R | I | E | H | K | S |
| A/Duck/Shanghai/1/2000 | H5 | AF501235 | 2000 | D | R | I | E | H | K | S |
| A/Goose/Huadong/1/2000 | H5N1 | DQ201829 | 2000 | D | R | I | E | H | K | S |
| A/Goose/Hong Kong/485.3/2000 | H5N1 | GU052042 | 2000 | D | R | I | E | H | K | S |
| A/Goose/Hong Kong/1032.6/2000 | H5N1 | GU052050 | 2000 | D | R | I | E | H | K | S |
| A/Duck/Zhejiang/5Z/2000 | H5N1 | AY585377 | 2000 | D | R | I | E | Q | K | S |
| A/Duck/Hong Kong/2986.12/2000 | H5N1 | GU052065 | 2000 | D | R | I | E | Q | K | S |
| A/Goose/Hong Kong/3014.5/2000 | H5N1 | AY075030 | 2000 | D | R | I | E | Q | K | S |

[a]* indicates that except for the mutation at position 107 (position 123), all other residues were established to confer higher virulence in reference 60.

Some HA virulence determinants could already be revealed by the determination of different 50% lethal dose ($LD_{50}$) values of closely related H5N1 HPAIV in chicken mutated at HA1 positions 97, 108, 126, 138, 212, and 217 (60) (corresponding to positions 113, 124, 142, 154, 228, and 233, respectively, in the full-length R65 HA translated sequence). All these residues are identical in the R65 HA and H5 HPAIV consensus sequence (determined from 3,385 sequences) but are different in the corresponding positions of the TG05 HA and LPAIV consensus sequence (from 803 sequences), except for the rather conserved residue 97 (residue 113) (Fig. 1). Among these mutations, HA 124I was attributed to increased acid sensitivity and virulence in chickens (37). Furthermore, sequence database searches revealed that both 123R and 124I are predominant as a dual motif in the overwhelming majority of 97.5% of H5 HPAIV, in contrast to H5 LPAIV. Remarkably, this dual motif is retained in later and contemporary H5 HPAIV, including novel H5NX reassortants, like the H5N8 or the H5N6 strains, which can cause experimental infections in dogs and zoonotic infections in humans (61–65).

However, a few HPAIV (2.0%) carry 123S and 124T or only a single exchange (up to 0.5%) (Fig. 2A). Among them, A/Duck/Guangxi/07/1999 (66) carries neither 123R, 124I, nor any of the candidate HA1 mutations established previously (60) (Table 3). Interestingly, this strain killed only two of seven oculonasally infected chickens without

**TABLE 4** Prevalence of amino acids 123 and 124 among H5 HPAIV clades[a]

| Mutation(s) and clade | Count (no. of sequences) | Fraction of sequences (%) |
|---|---|---|
| R123 and I124 | | |
| Found total | 961 | 100.0 |
| c0 | 48 | 5.0 |
| c1 | 99 | 10.3 |
| c1.1 | 15 | 1.6 |
| c1-8-like | 2 | 0.2 |
| c2.1.1 | 17 | 1.8 |
| c2.1.2 | 10 | 1.0 |
| c2.1.3 | 16 | 1.7 |
| c2.1.3.1 | 8 | 0.8 |
| c2.1.3.2 | 71 | 7.4 |
| c2.1.3.3 | 4 | 0.4 |
| c2.2 | 156 | 16.2 |
| c2.2.1 | 153 | 15.9 |
| c2.2.1.1 | 46 | 4.8 |
| c2.2.2 | 12 | 1.2 |
| c2.3.1 | 4 | 0.4 |
| c2.3.2 | 12 | 1.2 |
| c2.3.2.1 | 40 | 4.2 |
| c2.3.3 | 1 | 0.1 |
| c2.3.4 | 95 | 9.9 |
| c2.3.4.1 | 3 | 0.3 |
| c2.3.4.2 | 4 | 0.4 |
| c2.3.4.3 | 20 | 2.1 |
| c2.4 | 16 | 1.7 |
| c2.5 | 11 | 1.1 |
| c2-like | 4 | 0.4 |
| c3 | 15 | 1.6 |
| c3-like | 2 | 0.2 |
| c4 | 2 | 0.2 |
| c5 | 8 | 0.8 |
| c5-6-like | 5 | 0.5 |
| c6 | 6 | 0.6 |
| c7 | 23 | 2.4 |
| c7.1 | 9 | 0.9 |
| c7.2 | 8 | 0.8 |
| c8-9-like | 1 | 0.1 |
| c9 | 15 | 1.6 |
| R123 or I124 | | |
| Found total | 10 | 100.0 |
| c0 | 8 | 80.0 |
| c2.2.1.1 | 1 | 10.0 |
| c7 | 1 | 10.0 |
| S123 and T124 | | |
| Found total | 32 | 100.0 |
| Am_nonGsGD | 16 | 50.0 |
| EA_nonGsGD | 14 | 43.8 |
| c0 | 1 | 3.1 |
| c5-6-like | 1 | 3.1 |

[a]Survey for the 123R and 124I amino acids among 1,003 H5 sequences assigned to H5 clades (67) according to the LABEL algorithm (68). All clades which were found multiply are shaded.

systemic replication and was avirulent in mice (66). This observation supports the notion that the HA 123R/124I dual motif is crucial for high virulence in avian and mammalian hosts.

Furthermore, a survey for the HA 123R/124I motif among 1,003 H5 HPAIV sequences assigned to the H5 clades (67) by the LABEL algorithm (68) confirmed its absence among American and Eurasian non-Goose/Guangdong-like strains and its presence in all main H5 clades (Tables 4 and 5).

**TABLE 5** All known H5 HPAIV carrying neither 123R nor 124I

| Virus strain | Serotype | GenBank accession no. | Yr |
|---|---|---|---|
| A/Chicken/Scotland/1959 | H5N1 | GU052518 | 1959 |
| A/Tern/SouthAfrica/1961 | H5N3 | U20460 | 1961 |
| A/Turkey/Ontario/7732/1966 | H5N9 | AB558456 | 1966 |
| A/Chicken/Pennsylvania/1/1983 | H5N2 | CY015073 | 1983 |
| A/Chicken/Pennsylvania/1370/1983 | H5N2 | GU052771 | 1983 |
| A/Chicken/Pennsylvania/21525/1983 | H5N2 | GU052787 | 1983 |
| A/Duck/Ireland/113/1983 | H5N8 | M18450 | 1983 |
| A/Duck/Ireland/113/1983 | H5N8 | GU052853 | 1983 |
| A/Turkey/Ireland/1378/1983 | H5N8 | CY015089 | 1983 |
| A/Turkey/Ireland/1378/1983 | H5N8 | M18451 | 1983 |
| A/Chicken/VA/40018/1984 | H5N2 | FJ610134 | 1984 |
| A/Chicken/Florida/277162/1986 | H5N2 | GU052779 | 1986 |
| A/Chicken/Pennsylvania/10210/1986 | H5N2 | GU052747 | 1986 |
| A/Goose/OH/229112/1986 | H5N2 | EU743233 | 1986 |
| A/Guineafowl/OH/2291120/1986 | H5N2 | FJ357091 | 1986 |
| A/Turkey/England/50-92/1991 | H5N1 | GU052510 | 1991 |
| A/Chicken/Puebla/14587644/1994 | H5N2 | FJ610094 | 1994 |
| A/Chicken/Puebla/8623607/1994 | H5N2 | AB558473 | 1994 |
| A/Chicken/Queretaro/1458819/1995 | H5N2 | AB558474 | 1995 |
| A/Chicken/Italy/312/1997 | H5N2 | CY015115 | 1997 |
| A/Chicken/Italy/312/1997 | H5N2 | AF194169 | 1997 |
| A/Chicken/Italy/367/1997 | H5N2 | AF194990 | 1997 |
| A/Poultry/Italy/330/1997 | H5N2 | CY017403 | 1997 |
| A/Poultry/Italy/365/1997 | H5N2 | CY022261 | 1997 |
| A/Poultry/Italy/373/1997 | H5N2 | CY020229 | 1997 |
| A/Poultry/Italy/382/1997 | H5N2 | CY018949 | 1997 |
| A/Chicken/Italy/8/1998 | H5N2 | EF597267 | 1998 |
| A/Duck/Guangxi/07/1999 | H5N1 | AY585363 | 1999 |
| A/Chicken/Texas/1672804/2002 | H5N3 | CY034683 | 2002 |
| A/Duck/Zhejiang/Bj/2002 | H5N1 | DQ997410 | 2002 |
| A/Chicken/Taiwan/1209/2003 | H5N2 | AY573917 | 2003 |
| A/Chicken/Texas/2983132/2004 | H5N2 | GU052644 | 2004 |
| A/Chicken/TX/298313/2004 | H5N2 | AY849793 | 2004 |
| A/Ostrich/SouthAfrica/N227/2004 | H5N2 | FJ519983 | 2004 |
| A/Ostrich/SouthAfrica/AI1091/2006 | H5N2 | EF591749 | 2006 |
| A/Quail/NewYork/501360/2007 | H5N2 | GQ923549 | 2007 |
| A/Spurwingedgoose/Nigeria/53882/2007 | H5N2 | EU544248 | 2007 |
| A/Chicken/Taiwan/A7031/2008 | H5N2 | AB507264 | 2008 |
| A/Chicken/Taiwan/CHA1029/2010 | H5N2 | KY989969 | 2010 |
| A/Ostrich/SouthAfrica/AI2114/2011 | H5N2 | JX069081 | 2011 |
| A/Ostrich/SouthAfrica/AI2214/2011 | H5N2 | JX069089 | 2011 |
| A/Ostrich/SouthAfrica/AI2512/2011 | H5N2 | JX069097 | 2011 |
| A/Ostrich/South-Africa/1104333C/2011 | H5N2 | EPI371563 | 2011 |
| A/Ostrich/South-Africa/1104333A/2011 | H5N2 | EPI371562 | 2011 |
| A/Chicken/China/G2/2012 | H5N1 | KU851866 | 2012 |
| A/Chicken/Taiwan/0101/2012 | H5N2 | KF193386 | 2012 |
| A/Chicken/Taiwan/0502/2012 | H5N2 | KJ720208 | 2012 |
| A/Chicken/Taiwan/2593/2012 | H5N2 | KJ162612 | 2012 |
| A/Chicken/Taiwan/683/2012 | H5N2 | KJ162588 | 2012 |
| A/Chicken/Taiwan/689/2012 | H5N2 | KJ162596 | 2012 |
| A/Chicken/Taiwan/A1997/2012 | H5N2 | KF193394 | 2012 |
| A/Chicken/Taiwan/CYA2628/2012 | H5N2 | KY989967 | 2012 |
| A/Chicken/Taiwan/1692/2013 | H5N2 | KJ162636 | 2013 |
| A/Chicken/Taiwan/1680/2013 | H5N2 | KJ162620 | 2013 |
| A/Chicken/Taiwan/1711/2013 | H5N2 | KJ162652 | 2013 |
| A/Chicken/Taiwan/4443/2013 | H5N2 | KJ162708 | 2013 |
| A/Chicken/Taiwan/7350/2013 | H5N2 | KJ162668 | 2013 |
| A/Chicken/Taiwan/8988/2013 | H5N2 | KJ162676 | 2013 |
| A/Chicken/YL/A3190/2014 | H5N2 | KR137710 | 2014 |
| A/Chicken/CH/A556/2015 | H5N2 | KR137678 | 2015 |
| A/Chicken/France/150169a/2015 | H5N1 | KU310447 | 2015 |
| A/Chicken/GY/A451/2015 | H5N2 | KR137662 | 2015 |
| A/Chicken/PT/A158/2015 | H5N2 | KR137654 | 2015 |
| A/Chicken/SC/A688/2015 | H5N2 | KR137694 | 2015 |
| A/Chicken/TC/A504/2015 | H5N2 | KR137670 | 2015 |
| A/Chicken/TY/A665/2015 | H5N2 | KR137686 | 2015 |
| A/Duck/France/150233/2015 | H5N2 | KX014878 | 2015 |
| A/Guineafowl/France/150207n/2015 | H5N9 | KU320887 | 2015 |

Changes in the pH required for triggering HA-mediated fusion have been recognized as part of the process of adaptation of influenza viruses to novel hosts. Whereas human-adapted strains show a decrease in pH sensitivity (36), HPAIV display an increased fusion pH accompanied by increased virulence in chickens (37, 69) and enhanced replication in the upper respiratory tracts of mice and ferrets (70, 71). An

explanation for such divergent evolution could be that that both virus lineages undergo different selection pressures. In this regard, the demonstration that human strains primarily target nonciliated cells in the respiratory tract, whereas avian strains infect ciliated cells dependent on the virus receptor preference for $\alpha$2-6- or $\alpha$2-3-linked sialic acids (72), might suggest that the different cell populations exert different evolutionary pressures. Alternatively, it is tempting to speculate that the acidification of the endosome is enhanced by upregulated V-ATPase activity due to the early activation of extracellular signal-regulated kinase (ERK) and phosphatidylinositol 3-kinase (PI3K) by the virus (73). It remains to be elucidated whether differences in primary cellular tropism and/or virus-mediated regulation of the endosomal pH determine the different evolutionary pathways of avian and human virus lineages. Remarkably, the earliest H5N1 HPAIV strains from 1996/1997 (74, 75), A/Goose/Guangdong/1/1996 (76) and A/Goose/Guangdong/3/1997, carry only the HA 123R mutation but neither 124I nor any of the other identified HA1 residues relevant for virulence (60). Therefore, 123R was crucial in early H5 HPAIV evolution, whereas 124I was acquired later in the clade 0 viruses from 1997, as seen in the first known chicken isolate, A/Chicken/Hong Kong/220/1997 (77). Later on, other HA1 exchanges (60) also appeared: 126E (142E) and 217S (233S) in 1997 and then 212K (228K) in 2000. Eventually, 138N (154N) complemented the whole set of all six key positions in the 2000 HPAIV (Table 3).

Because several cell lines and tissues display different final (minimum) pH in their endosomes (78, 79), they may not be permissible to influenza virus infection if the required HA fusion activation pH of a particular strain is lower than the endosomal endpoint pH, as is the case with LPAIV (54, 78). Therefore, an increased acid sensitivity of the HA activating fusion competence enables the virus to infect cells with a milder acidic final pH in their endosomes, resulting in extended cell tropism (78, 79). To this end, the RI motif at HA positions 123 and 124, in addition to the polybasic HACS, may serve as a door opener to the respiratory tract for H5 HPAIV (70, 78, 79).

Taken together, the HA 123R/124I dual motif is crucial for high virulence in avian and mammalian hosts, indicating substantial relevance for the high zoonotic potential of H5 HPAIV. Accordingly, this virulence determinant is still predominant in Asian H5 HPAIV, including the novel H5NX reassortants. For HPAIV emergence, the acquisition of the polybasic HACS is the critical step but requires parallel coadaptation of the HA. The HA 123R/124I dual motif leads to an increased acid sensitivity, allowing broader viral tissue tropism for cells with an elevated (less-acidic) endpoint pH in their endosomes (78, 79). This acquired gain of function might enable HPAIV to infect the respiratory tract of avian and mammalian hosts (37, 70, 71, 79) and therefore facilitate zoonotic spillover infections. Whether such an adaptation would result in dead-end evolution compared to established human strains or airborne-transmissible H5N1 HPAIV mutants requiring sensitivity to lower pH (36, 57, 80, 81) remains elusive.

Overall, we propose that, in addition to the acquisition of a polybasic HACS, the coadaptation of the HA to sensitivity to higher pH results in a broader viral organ tropism extended to the respiratory tract, enabling the emergence of novel HPAIV.

## MATERIALS AND METHODS

**Sequence database surveys.** On 24 July 2017, we downloaded all available H5 protein sequences from fluDB (38) and GISAID (https://www.gisaid.org/) (an acknowledgment spreadsheet of all laboratories contributing to GISAID is available upon request) and performed an alignment by using the MAFFT algorithm (82) implemented in the Geneious package (83). For further analysis, we removed all duplicated, truncated, or gapped sequences. Sequence positions refer to the R65 HA sequence, including the signal peptide (16 amino acids).

**Cells and recombinant viruses.** Human embryonic kidney (293T), Madin-Darby canine kidney (MDCK), and baby hamster kidney (BHK-21) cells were maintained in Dulbecco's modified Eagle's medium (DMEM) containing 10% fetal calf serum (FCS), whereas chicken fibroblast cells (DF1) were cultured in Iscove's DMEM plus 10% FCS.

The recombinant H5N1 HPAIV A/Swan/Germany/R65/06 (R65) (GenBank accession numbers DQ464354 to DQ464361) was grown in MDCK cells, and the existence of unwanted mutations was excluded by Sanger sequencing (18). $TG05_{poly}$, a polybasic HACS mutant from H5N1 LPAIV A/Teal/Germany/Wv632/2005 (18), was propagated in 11-day-old embryonated chicken eggs. Chimeric HA from R65 and $TG05_{poly}$ were assembled by target-primed plasmid amplification (39); HA single point mutants

were obtained by QuikChange site-directed mutagenesis (primer sequences are available upon request). The mutants were rescued as described previously (84) and then propagated in MDCK cells; virus gene compositions and full-length HA genes were verified by Sanger sequencing of reverse transcription-PCR (RT-PCR) amplicons. All viruses were handled under biosafety level 3 plus ($BSL3^+$) conditions.

**Plaque assay and growth curves.** For plaque assays, we infected MDCK cells, as described previously (85), with 400 $\mu$l virus inoculum in the absence of trypsin. For growth curves, we inoculated DF1 cells at a multiplicity of infection (MOI) of 0.001. From two independent replicates, we harvested supernatants 0, 24, 48, and 72 h after inoculation for titration by plaque assays (85).

**Animal experiments.** The animal experiments were evaluated by the responsible ethics committee of the State Office for Agriculture, Food Safety, and Fishery in Mecklenburg-Western Pomerania (LALFF M-V) and gained governmental approval (registration numbers LALLF M-V/TSD/7221.3-1.1-018/07 and LALLF M-V/TSD/7221.3-1.1-023/13). We infected 2-week-old White Leghorn specific-pathogen-free chickens (three or six per group) oculonasally at a dosage of $10^5$ PFU. For transmission studies, we added four contact animals at 1 day p.i. Each bird was observed daily for 10 days for clinical signs and classified according to OIE criteria; moribund birds were killed and scored as dead on the next observation day (86). Sera of surviving birds were collected at day 10 and tested for influenza A virus nucleoprotein-specific antibodies by a competitive enzyme-linked immunosorbent assay (ELISA) (ID-Vet), as recommended by the manufacturer.

Four-week-old female BALB/c mice (Charles River, Sulzfeld, Germany) were housed in ISOcages (Tecniplast, Buguggiate, Italy). After anesthesia by isoflurane inhalation, we intranasally inoculated the animals with 30 $\mu$l phosphate-buffered saline (PBS) (mock) or PBS-diluted virus at a dosage of $10^5$ PFU. Over a period of 14 days, we observed each mouse daily regarding body weight changes, other clinical symptoms, or death. By a plaque assay, we titrated entire organ homogenates of lungs, hearts, and brains from inoculated mice, sacrificed at 3 days p.i.

**Thermal stability.** In two independent experiments, we incubated the viruses in a thermoblock for 30 min at 4°C, 37°C, 42°C, or 50°C prior to hemagglutination assay at room temperature using 1% chicken red blood cells.

**Syncytium formation assays.** BHK-21 monolayers in six-well plates were infected at an MOI of 2 and incubated at 37°C for 30 min. We then washed the cells with PBS and overlaid them with DMEM containing 0.2% bovine serum albumin (BSA) and antibiotics. After 6 h, the cells were incubated at 37°C for 5 min in PBS in parallel at different pH adjusted in 0.1-unit increments from 4.8 to 6.0. We then washed the cells, incubated them in DMEM containing 10% FCS at 37°C 2 h, and stained them eventually with a Hema-3 Stat Pack staining kit (Fisher, USA). We noted the fusion activation pH as the highest pH sufficient for the formation of any syncytia.

**Virus inactivation pH.** First, we incubated DF1 cells for 30 min at 37°C in parallel with virus at an MOI of 2 diluted in PBS at different pH adjusted in 0.1-unit increments from 4.0 to 6.0. After the removal of the inoculum, we kept the cells in Iscove's DMEM containing BSA (0.2%) and antibiotics at 37°C for 5 h. Cells were then fixed with 3.7% formaldehyde (Roth, Germany), permeabilized with 0.5% Triton X-100 (Merck, Germany), and blocked for 30 min with 1% skim milk in PBS. Infected cells were stained with a polyclonal antibody to the NP protein from A/WSN/1933 (H1N1) (1:1,000; incubated for 1 h at room temperature) (GeneTex, USA) and washed with PBS three times prior to detection with goat anti-rabbit Alexa Fluor 488 antibody (Invitrogen, Germany) by fluorescence microscopy. All experiments were done in duplicates. The highest pH at which no virus-infected cells were found was designated the virus inactivation pH.

## ACKNOWLEDGMENTS

We thank Stephanie Peitsch, Mandy Schmidt, Doreen Fiedler, and Frank Klipp for skillful technical assistance and animal caretaking. We acknowledge the authors and the originating and submitting laboratories of the sequences from GISAID's EpiFlu Database on which this research is based (GISAID acknowledgment table is available upon request).

This work was supported by the Deutsche Forschungsgemeinschaft (DFG) (STE 1957/1-1).

## REFERENCES

1. Neumann G, Chen H, Gao GF, Shu Y, Kawaoka Y. 2010. H5N1 influenza viruses: outbreaks and biological properties. Cell Res 20:51–61. https://doi.org/10.1038/cr.2009.124.
2. Capua I, Marangon S. 2000. The avian influenza epidemic in Italy, 1999-2000: a review. Avian Pathol 29:289–294. https://doi.org/10.1080/03079450050118403.
3. Fouchier RA, Schneeberger PM, Rozendaal FW, Broekman JM, Kemink SA, Munster V, Kuiken T, Rimmelzwaan GF, Schutten M, Van Doornum GJ, Koch G, Bosman A, Koopmans M, Osterhaus AD. 2004. Avian influenza A virus (H7N7) associated with human conjunctivitis and a fatal case of acute respiratory distress syndrome. Proc Natl Acad Sci U S A 101:1356–1361. https://doi.org/10.1073/pnas.0308352100.
4. Kawaoka Y, Webster RG. 1985. Evolution of the A/Chicken/Pennsylvania/83 (H5N2) influenza virus. Virology 146:130–137. https://doi.org/10.1016/0042-6822(85)90059-5.
5. Suarez DL, Senne DA, Banks J, Brown IH, Essen SC, Lee CW, Manvell RJ, Mathieu-Benson C, Moreno V, Pedersen JC, Panigrahy B, Rojas H, Spackman E, Alexander DJ. 2004. Recombination resulting in virulence shift in avian influenza outbreak, Chile. Emerg Infect Dis 10:693–699. https://doi.org/10.3201/eid1004.030396.
6. Bosch FX, Garten W, Klenk HD, Rott R. 1981. Proteolytic cleavage of influenza virus hemagglutinins: primary structure of the connecting peptide between HA1 and HA2 determines proteolytic cleavability and pathogenicity of avian influenza viruses. Virology 113:725–735. https://doi.org/10.1016/0042-6822(81)90201-4.
7. Bosch FX, Orlich M, Klenk HD, Rott R. 1979. The structure of the hem-

agglutinin, a determinant for the pathogenicity of influenza viruses. Virology 95:197–207. https://doi.org/10.1016/0042-6822(79)90414-8.
8. Senne DA, Panigrahy B, Kawaoka Y, Pearson JE, Suss J, Lipkind M, Kida H, Webster RG. 1996. Survey of the hemagglutinin (HA) cleavage site sequence of H5 and H7 avian influenza viruses: amino acid sequence at the HA cleavage site as a marker of pathogenicity potential. Avian Dis 40:425–437. https://doi.org/10.2307/1592241.
9. Huang RTC, Wahn K, Klenk HD, Rott R. 1980. Fusion between cell membranes and liposomes containing the glycoprotein of influenza virus. Virology 104:294–302. https://doi.org/10.1016/0042-6822(80)90334-7.
10. Klenk HD, Rott R, Orlich M, Blodorn J. 1975. Activation of influenza A viruses by trypsin treatment. Virology 68:426–439. https://doi.org/10.1016/0042-6822(75)90284-6.
11. Lazarowitz SG, Choppin PW. 1975. Enhancement of the infectivity of influenza A and B viruses by proteolytic cleavage of the hemagglutinin polypeptide. Virology 68:440–454. https://doi.org/10.1016/0042-6822(75)90285-8.
12. Bottcher-Friebertshauser E, Klenk HD, Garten W. 2013. Activation of influenza viruses by proteases from host cells and bacteria in the human airway epithelium. Pathog Dis 69:87–100. https://doi.org/10.1111/2049-632X.12053.
13. Stieneke-Groeber A, Vey M, Angliker H, Shaw E, Thomas G, Roberts C, Klenk HD, Garten W. 1992. Influenza virus hemagglutinin with multibasic cleavage site is activated by furin, a subtilisin-like endoprotease. EMBO J 11:2407–2414.
14. Wong SS, Yoon SW, Zanin M, Song MS, Oshansky C, Zaraket H, Sonnberg S, Rubrum A, Seiler P, Ferguson A, Krauss S, Cardona C, Webby RJ, Crossley B. 2014. Characterization of an H4N2 influenza virus from quails with a multibasic motif in the hemagglutinin cleavage site. Virology 468–470:72–80. https://doi.org/10.1016/j.virol.2014.07.048.
15. Gohrbandt S, Veits J, Breithaupt A, Hundt J, Teifke JP, Stech O, Mettenleiter TC, Stech J. 2011. H9 avian influenza reassortant with engineered polybasic cleavage site displays a highly pathogenic phenotype in chicken. J Gen Virol 92:1843–1853. https://doi.org/10.1099/vir.0.031591-0.
16. Horimoto T, Kawaoka Y. 1994. Reverse genetics provides direct evidence for a correlation of hemagglutinin cleavability and virulence of an avian influenza A virus. J Virol 68:3120–3128.
17. Gohrbandt S, Veits J, Hundt J, Bogs J, Breithaupt A, Teifke JP, Weber S, Mettenleiter TC, Stech J. 2011. Amino acids adjacent to the haemagglutinin cleavage site are relevant for virulence of avian influenza viruses of subtype H5. J Gen Virol 92:51–59. https://doi.org/10.1099/vir.0.023887-0.
18. Bogs J, Veits J, Gohrbandt S, Hundt J, Stech O, Breithaupt A, Teifke JP, Mettenleiter TC, Stech J. 2010. Highly pathogenic H5N1 influenza viruses carry virulence determinants beyond the polybasic hemagglutinin cleavage site. PLoS One 5:e11826. https://doi.org/10.1371/journal.pone.0011826.
19. Munster VJ, Schrauwen EJ, de Wit E, van den Brand JM, Bestebroer TM, Herfst S, Rimmelzwaan GF, Osterhaus AD, Fouchier RA. 2010. Insertion of a multibasic cleavage motif into the hemagglutinin of a low-pathogenic avian influenza H6N1 virus induces a highly pathogenic phenotype. J Virol 84:7953–7960. https://doi.org/10.1128/JVI.00449-10.
20. Stech O, Veits J, Weber S, Deckers D, Schroer D, Vahlenkamp TW, Breithaupt A, Teifke J, Mettenleiter TC, Stech J. 2009. Acquisition of a polybasic hemagglutinin cleavage site by a low-pathogenic avian influenza virus is not sufficient for immediate transformation into a highly pathogenic strain. J Virol 83:5864–5868. https://doi.org/10.1128/JVI.02649-08.
21. Veits J, Weber S, Stech O, Breithaupt A, Graber M, Gohrbandt S, Bogs J, Hundt J, Teifke JP, Mettenleiter TC, Stech J. 2012. Avian influenza virus hemagglutinins H2, H4, H8, and H14 support a highly pathogenic phenotype. Proc Natl Acad Sci U S A 109:2579–2584. https://doi.org/10.1073/pnas.1109397109.
22. Abdelwhab SM, Veits J, Breithaupt A, Gohrbandt S, Ziller M, Teifke JP, Stech J, Mettenleiter TC. 2016. Prevalence of the C-terminal truncations of NS1 in avian influenza A viruses and effect on virulence and replication of a highly pathogenic H7N1 virus in chickens. Virulence 7:546–557. https://doi.org/10.1080/21505594.2016.1159367.
23. Stech O, Veits J, Abdelwhab E-SM, Wessels U, Mettenleiter TC, Stech J. 2015. The neuraminidase stalk deletion serves as major virulence determinant of H5N1 highly pathogenic avian influenza viruses in chicken. Sci Rep 5:13493. https://doi.org/10.1038/srep13493.
24. Wasilenko JL, Lee CW, Sarmento L, Spackman E, Kapczynski DR, Suarez DL, Pantin-Jackwood MJ. 2008. NP, PB1, and PB2 viral genes contribute to altered replication of H5N1 avian influenza viruses in chickens. J Virol 82:4544–4553. https://doi.org/10.1128/JVI.02642-07.
25. Munier S, Larcher T, Cormier-Aline F, Soubieux D, Su B, Guigand L, Labrosse B, Cherel Y, Quere P, Marc D, Naffakh N. 2010. A genetically engineered waterfowl influenza virus with a deletion in the stalk of the neuraminidase has increased virulence for chickens. J Virol 84:940–952. https://doi.org/10.1128/JVI.01581-09.
26. Sorrell EM, Song H, Pena L, Perez DR. 2010. A 27-amino-acid deletion in the neuraminidase stalk supports replication of an avian H2N2 influenza A virus in the respiratory tract of chickens. J Virol 84:11831–11840. https://doi.org/10.1128/JVI.01460-10.
27. Li Y, Chen S, Zhang X, Fu Q, Zhang Z, Shi S, Zhu Y, Gu M, Peng D, Liu X. 2014. A 20-amino-acid deletion in the neuraminidase stalk and a five-amino-acid deletion in the NS1 protein both contribute to the pathogenicity of H5N1 avian influenza viruses in mallard ducks. PLoS One 9:e95539. https://doi.org/10.1371/journal.pone.0095539.
28. Li Z, Jiang Y, Jiao P, Wang A, Zhao F, Tian G, Wang X, Yu K, Bu Z, Chen H. 2006. The NS1 gene contributes to the virulence of H5N1 avian influenza viruses. J Virol 80:11115–11123. https://doi.org/10.1128/JVI.00993-06.
29. Connor RJ, Kawaoka Y, Webster RG, Paulson JC. 1994. Receptor specificity in human, avian, and equine H2 and H3 influenza virus isolates. Virology 205:17–23. https://doi.org/10.1006/viro.1994.1615.
30. Matrosovich M, Tuzikov A, Bovin N, Gambaryan A, Klimov A, Castrucci MR, Donatelli I, Kawaoka Y. 2000. Early alterations of the receptor-binding properties of H1, H2, and H3 avian influenza virus hemagglutinins after their introduction into mammals. J Virol 74:8502–8512. https://doi.org/10.1128/JVI.74.18.8502-8512.2000.
31. Rogers GN, Paulson JC. 1983. Receptor determinants of human and animal influenza virus isolates: differences in receptor specificity of the H3 hemagglutinin based on species of origin. Virology 127:361–373. https://doi.org/10.1016/0042-6822(83)90150-2.
32. Rogers GN, Paulson JC, Daniels RS, Skehel JJ, Wilson IA, Wiley DC. 1983. Single amino acid substitutions in influenza haemagglutinin change receptor binding specificity. Nature 304:76–78. https://doi.org/10.1038/304076a0.
33. Maeda T, Ohnishi S. 1980. Activation of influenza virus by acidic media causes hemolysis and fusion of erythrocytes. FEBS Lett 122:283–287. https://doi.org/10.1016/0014-5793(80)80457-1.
34. White JM, Matlin K, Helenius A. 1981. Cell fusion by Semliki Forest, influenza, and vesicular stomatitis viruses. J Cell Biol 89:674–679. https://doi.org/10.1083/jcb.89.3.674.
35. Skehel JJ, Wiley DC. 2000. Receptor binding and membrane fusion in virus entry: the influenza hemagglutinin. Annu Rev Biochem 69:531–569. https://doi.org/10.1146/annurev.biochem.69.1.531.
36. Russier M, Yang G, Rehg JE, Wong SS, Mostafa HH, Fabrizio TP, Barman S, Krauss S, Webster RG, Webby RJ, Russell CJ. 2016. Molecular requirements for a pandemic influenza virus: an acid-stable hemagglutinin protein. Proc Natl Acad Sci U S A 113:1636–1641. https://doi.org/10.1073/pnas.1524384113.
37. DuBois RM, Zaraket H, Reddivari M, Heath RJ, White SW, Russell CJ. 2011. Acid stability of the hemagglutinin protein regulates H5N1 influenza virus pathogenicity. PLoS Pathog 7:e1002398. https://doi.org/10.1371/journal.ppat.1002398.
38. Zhang Y, Aevermann BD, Anderson TK, Burke DF, Dauphin G, Gu Z, He S, Kumar S, Larsen CN, Lee AJ, Li X, Macken C, Mahaffey C, Pickett BE, Reardon B, Smith T, Stewart L, Suloway C, Sun G, Tong L, Vincent AL, Walters B, Zaremba S, Zhao H, Zhou L, Zmasek C, Klem EB, Scheuermann RH. 2017. Influenza Research Database: an integrated bioinformatics resource for influenza virus research. Nucleic Acids Res 45:D466–D474. https://doi.org/10.1093/nar/gkw857.
39. Stech J, Stech O, Herwig A, Altmeppen H, Hundt J, Gohrbandt S, Kreibich A, Weber S, Klenk HD, Mettenleiter TC. 2008. Rapid and reliable universal cloning of influenza A virus genes by target-primed plasmid amplification. Nucleic Acids Res 36:e139. https://doi.org/10.1093/nar/gkn646.
40. Gao Y, Zhang Y, Shinya K, Deng G, Jiang Y, Li Z, Guan Y, Tian G, Li Y, Shi J, Liu L, Zeng X, Bu Z, Xia X, Kawaoka Y, Chen H. 2009. Identification of amino acids in HA and PB2 critical for the transmission of H5N1 avian influenza viruses in a mammalian host. PLoS Pathog 5:e1000709. https://doi.org/10.1371/journal.ppat.1000709.
41. Suptawiwat O, Boonarkart C, Chakritbudsabong W, Uiprasertkul M, Puthavathana P, Wiriyarat W, Auewarakul P. 2015. The N-linked glycosylation site at position 158 on the head of hemagglutinin and the

virulence of H5N1 avian influenza virus in mice. Arch Virol 160:409–415. https://doi.org/10.1007/s00705-014-2306-x.
42. Acharya R, Carnevale V, Fiorin G, Levine BG, Polishchuk AL, Balannik V, Samish I, Lamb RA, Pinto LH, DeGrado WF, Klein ML. 2010. Structure and mechanism of proton transport through the transmembrane tetrameric M2 protein bundle of the influenza A virus. Proc Natl Acad Sci U S A 107:15075–15080. https://doi.org/10.1073/pnas.1007071107.
43. Betakova T, Ciampor F, Hay AJ. 2005. Influence of residue 44 on the activity of the M2 proton channel of influenza A virus. J Gen Virol 86:181–184. https://doi.org/10.1099/vir.0.80358-0.
44. Schnell JR, Chou JJ. 2008. Structure and mechanism of the M2 proton channel of influenza A virus. Nature 451:591–595. https://doi.org/10.1038/nature06531.
45. Stouffer AL, Acharya R, Salom D, Levine AS, Di Costanzo L, Soto CS, Tereshko V, Nanda V, Stayrook S, DeGrado WF. 2008. Structural basis for the function and inhibition of an influenza virus proton channel. Nature 451:596–599. https://doi.org/10.1038/nature06528.
46. Carr CM, Chaudhry C, Kim PS. 1997. Influenza hemagglutinin is spring-loaded by a metastable native conformation. Proc Natl Acad Sci U S A 94:14306–14313.
47. Xu R, Wilson IA. 2011. Structural characterization of an early fusion intermediate of influenza virus hemagglutinin. J Virol 85:5172–5182. https://doi.org/10.1128/JVI.02430-10.
48. Ha Y, Stevens DJ, Skehel JJ, Wiley DC. 2001. X-ray structures of H5 avian and H9 swine influenza virus hemagglutinins bound to avian and human receptor analogs. Proc Natl Acad Sci U S A 98:11181–11186. https://doi.org/10.1073/pnas.201401198.
49. Ha Y, Stevens DJ, Skehel JJ, Wiley DC. 2002. H5 avian and H9 swine influenza virus haemagglutinin structures: possible origin of influenza subtypes. EMBO J 21:865–875. https://doi.org/10.1093/emboj/21.5.865.
50. Shore DA, Yang H, Balish AL, Shepard SS, Carney PJ, Chang JC, Davis CT, Donis RO, Villanueva JM, Klimov AI, Stevens J. 2013. Structural and antigenic variation among diverse clade 2 H5N1 viruses. PLoS One 8:e75209. https://doi.org/10.1371/journal.pone.0075209.
51. Stevens J, Blixt O, Tumpey TM, Taubenberger JK, Paulson JC, Wilson IA. 2006. Structure and receptor specificity of the hemagglutinin from an H5N1 influenza virus. Science 312:404–410. https://doi.org/10.1126/science.1124513.
52. Xiong X, Coombs PJ, Martin SR, Liu J, Xiao H, McCauley JW, Locher K, Walker PA, Collins PJ, Kawaoka Y, Skehel JJ, Gamblin SJ. 2013. Receptor binding by a ferret-transmissible H5 avian influenza virus. Nature 497:392–396. https://doi.org/10.1038/nature12144.
53. Starick E, Beer M, Hoffmann B, Staubach C, Werner O, Globig A, Strebelow G, Grund C, Durban M, Conraths FJ, Mettenleiter T, Harder T. 2008. Phylogenetic analyses of highly pathogenic avian influenza virus isolates from Germany in 2006 and 2007 suggest at least three separate introductions of H5N1 virus. Vet Microbiol 128:243–252. https://doi.org/10.1016/j.vetmic.2007.10.012.
54. Okamatsu M, Motohashi Y, Hiono T, Tamura T, Nagaya K, Matsuno K, Sakoda Y, Kida H. 2016. Is the optimal pH for membrane fusion in host cells by avian influenza viruses related to host range and pathogenicity? Arch Virol 161:2235–2242. https://doi.org/10.1007/s00705-016-2902-z.
55. Chizhmakov IV, Ogden DC, Geraghty FM, Hayhurst A, Skinner A, Betakova T, Hay AJ. 2003. Differences in conductance of M2 proton channels of two influenza viruses at low and high pH. J Physiol 546:427–438. https://doi.org/10.1113/jphysiol.2002.028910.
56. Ciampor F, Thompson CA, Grambas S, Hay AJ. 1992. Regulation of pH by the M2 protein of influenza A viruses. Virus Res 22:247–258. https://doi.org/10.1016/0168-1702(92)90056-F.
57. Imai M, Watanabe T, Hatta M, Das SC, Ozawa M, Shinya K, Zhong G, Hanson A, Katsura H, Watanabe S, Li C, Kawakami E, Yamada S, Kiso M, Suzuki Y, Maher EA, Neumann G, Kawaoka Y. 2012. Experimental adaptation of an influenza H5 HA confers respiratory droplet transmission to a reassortant H5 HA/H1N1 virus in ferrets. Nature 486:420–428. https://doi.org/10.1038/nature10831.
58. Zhou J, Sun W, Wang J, Guo J, Yin W, Wu N, Li L, Yan Y, Liao M, Huang Y, Luo K, Jiang X, Chen H. 2009. Characterization of the H5N1 highly pathogenic avian influenza virus derived from wild pikas in China. J Virol 83:8957–8964. https://doi.org/10.1128/JVI.00793-09.
59. Bogs J, Kalthoff D, Veits J, Pavlova S, Schwemmle M, Manz B, Mettenleiter TC, Stech J. 2011. Reversion of PB2-627E to -627K during replication of an H5N1 clade 2.2 virus in mammalian hosts depends on the origin of the nucleoprotein. J Virol 85:10691–10698. https://doi.org/10.1128/JVI.00786-11.
60. Hulse DJ, Webster RG, Russell RJ, Perez DR. 2004. Molecular determinants within the surface proteins involved in the pathogenicity of H5N1 influenza viruses in chickens. J Virol 78:9954–9964. https://doi.org/10.1128/JVI.78.18.9954-9964.2004.
61. de Vries E, Guo H, Dai M, Rottier PJ, van Kuppeveld FJ, de Haan CA. 2015. Rapid emergence of highly pathogenic avian influenza subtypes from a subtype H5N1 hemagglutinin variant. Emerg Infect Dis 21:842–846. https://doi.org/10.3201/eid2105.141927.
62. Guo H, de Vries E, McBride R, Dekkers J, Peng W, Bouwman KM, Nycholat C, Verheije MH, Paulson JC, van Kuppeveld FJ, de Haan CA. 2017. Highly pathogenic influenza A(H5Nx) viruses with altered H5 receptor-binding specificity. Emerg Infect Dis 23:220–231. https://doi.org/10.3201/eid2302.161072.
63. Shen YY, Ke CW, Li Q, Yuan RY, Xiang D, Jia WX, Yu YD, Liu L, Huang C, Qi WB, Sikkema R, Wu J, Koopmans M, Liao M. 2016. Novel reassortant avian influenza A(H5N6) viruses in humans, Guangdong, China, 2015. Emerg Infect Dis 22:1507–1509. https://doi.org/10.3201/eid2208.160146.
64. Sun H, Pu J, Wei Y, Sun Y, Hu J, Liu L, Xu G, Gao W, Li C, Zhang X, Huang Y, Chang KC, Liu X, Liu J. 2016. Highly pathogenic avian influenza H5N6 viruses exhibit enhanced affinity for human type sialic acid receptor and in-contact transmission in model ferrets. J Virol 90:6235–6243. https://doi.org/10.1128/JVI.00127-16.
65. Lyoo KS, Na W, Phan LV, Yoon SW, Yeom M, Song D, Jeong DG. 11 October 2017. Experimental infection of clade 1.1.2 (H5N1), clade 2.3.2.1c (H5N1) and clade 2.3.4.4 (H5N6) highly pathogenic avian influenza viruses in dogs. Transbound Emerg Dis https://doi.org/10.1111/tbed.12731.
66. Chen H, Deng G, Li Z, Tian G, Li Y, Jiao P, Zhang L, Liu Z, Webster RG, Yu K. 2004. The evolution of H5N1 influenza viruses in ducks in southern China. Proc Natl Acad Sci U S A 101:10452–10457. https://doi.org/10.1073/pnas.0403212101.
67. Smith GJ, Donis RO, World Health Organization/World Organisation for Animal Health/Food and Agriculture Organization H5 Evolution Working Group. 2015. Nomenclature updates resulting from the evolution of avian influenza A(H5) virus clades 2.1.3.2a, 2.2.1, and 2.3.4 during 2013-2014. Influenza Other Respir Viruses 9:271–276. https://doi.org/10.1111/irv.12324.
68. Shepard SS, Davis CT, Bahl J, Rivailler P, York IA, Donis RO. 2014. LABEL: fast and accurate lineage assignment with assessment of H5N1 and H9N2 influenza A hemagglutinins. PLoS One 9:e86921. https://doi.org/10.1371/journal.pone.0086921.
69. Reed ML, Bridges OA, Seiler P, Kim JK, Yen HL, Salomon R, Govorkova EA, Webster RG, Russell CJ. 2010. The pH of activation of the hemagglutinin protein regulates H5N1 influenza virus pathogenicity and transmissibility in ducks. J Virol 84:1527–1535. https://doi.org/10.1128/JVI.02069-09.
70. Zaraket H, Bridges OA, Duan S, Baranovich T, Yoon SW, Reed ML, Salomon R, Webby RJ, Webster RG, Russell CJ. 2013. Increased acid stability of the hemagglutinin protein enhances H5N1 influenza virus growth in the upper respiratory tract but is insufficient for transmission in ferrets. J Virol 87:9911–9922. https://doi.org/10.1128/JVI.01175-13.
71. Zaraket H, Bridges OA, Russell CJ. 2013. The pH of activation of the hemagglutinin protein regulates H5N1 influenza virus replication and pathogenesis in mice. J Virol 87:4826–4834. https://doi.org/10.1128/JVI.03110-12.
72. Matrosovich MN, Matrosovich TY, Gray T, Roberts NA, Klenk HD. 2004. Human and avian influenza viruses target different cell types in cultures of human airway epithelium. Proc Natl Acad Sci U S A 101:4620–4624. https://doi.org/10.1073/pnas.0308001101.
73. Marjuki H, Gornitzky A, Marathe BM, Ilyushina NA, Aldridge JR, Desai G, Webby RJ, Webster RG. 2011. Influenza A virus-induced early activation of ERK and PI3K mediates V-ATPase-dependent intracellular pH change required for fusion. Cell Microbiol 13:587–601. https://doi.org/10.1111/j.1462-5822.2010.01556.x.
74. WHO/OIE/FAO/H5N1 Evolution Working Group. 2008. Toward a unified nomenclature system for highly pathogenic avian influenza virus (H5N1). Emerg Infect Dis 14:e1. https://doi.org/10.3201/eid1407.071681.
75. Zhou NN, Shortridge KF, Claas EC, Krauss SL, Webster RG. 1999. Rapid evolution of H5N1 influenza viruses in chickens in Hong Kong. J Virol 73:3366–3374.
76. Xu X, Subbarao K, Cox NJ, Guo Y. 1999. Genetic characterization of the pathogenic influenza A/Goose/Guangdong/1/96 (H5N1) virus: similarity of its hemagglutinin gene to those of H5N1 viruses from the 1997 outbreaks in Hong Kong. Virology 261:15–19. https://doi.org/10.1006/viro.1999.9820.

77. Suarez DL, Perdue ML, Cox N, Rowe T, Bender C, Huang J, Swayne DE. 1998. Comparisons of highly virulent H5N1 influenza A viruses isolated from humans and chickens from Hong Kong. J Virol 72:6678–6688.
78. Daidoji T, Watanabe Y, Arai Y, Kajikawa J, Hirose R, Nakaya T. 2017. Unique infectious strategy of H5N1 avian influenza virus is governed by the acid-destabilized property of hemagglutinin. Viral Immunol 30:398–407. https://doi.org/10.1089/vim.2017.0020.
79. Daidoji T, Watanabe Y, Ibrahim MS, Yasugi M, Maruyama H, Masuda T, Arai F, Ohba T, Honda A, Ikuta K, Nakaya T. 2015. Avian influenza virus infection of immortalized human respiratory epithelial cells depends upon a delicate balance between hemagglutinin acid stability and endosomal pH. J Biol Chem 290:10627–10642. https://doi.org/10.1074/jbc.M114.611327.
80. Russier M, Yang G, Marinova-Petkova A, Vogel P, Kaplan BS, Webby RJ, Russell CJ. 2017. H1N1 influenza viruses varying widely in hemagglutinin stability transmit efficiently from swine to swine and to ferrets. PLoS Pathog 13:e1006276. https://doi.org/10.1371/journal.ppat.1006276.
81. Linster M, van Boheemen S, de Graaf M, Schrauwen EJA, Lexmond P, Manz B, Bestebroer TM, Baumann J, van Riel D, Rimmelzwaan GF, Osterhaus A, Matrosovich M, Fouchier RAM, Herfst S. 2014. Identification, characterization, and natural selection of mutations driving airborne transmission of A/H5N1 virus. Cell 157:329–339. https://doi.org/10.1016/j.cell.2014.02.040.
82. Katoh K, Misawa K, Kuma K, Miyata T. 2002. MAFFT: a novel method for rapid multiple sequence alignment based on fast Fourier transform. Nucleic Acids Res 30:3059–3066. https://doi.org/10.1093/nar/gkf436.
83. Kearse M, Moir R, Wilson A, Stones-Havas S, Cheung M, Sturrock S, Buxton S, Cooper A, Markowitz S, Duran C, Thierer T, Ashton B, Meintjes P, Drummond A. 2012. Geneious Basic: an integrated and extendable desktop software platform for the organization and analysis of sequence data. Bioinformatics 28:1647–1649. https://doi.org/10.1093/bioinformatics/bts199.
84. Hoffmann E, Neumann G, Kawaoka Y, Hobom G, Webster RG. 2000. A DNA transfection system for generation of influenza A virus from eight plasmids. Proc Natl Acad Sci U S A 97:6108–6113. https://doi.org/10.1073/pnas.100133697.
85. Stech J, Xiong X, Scholtissek C, Webster RG. 1999. Independence of evolutionary and mutational rates after transmission of avian influenza viruses to swine. J Virol 73:1878–1884.
86. Alexander DJ. 2008. Manual of diagnostic tests & vaccines for terrestrial animals, p 465–481. *In* Vallat B (ed), Avian influenza, 6th ed. Office International des Epizooties, Paris, France.
87. Ni F, Chen X, Shen J, Wang Q. 2014. Structural insights into the membrane fusion mechanism mediated by influenza virus hemagglutinin. Biochemistry 53:846–854. https://doi.org/10.1021/bi401525h.